# STUDYING DOPA ADHESION ON POLYSTYRENE UNDER WATER

**A Thesis Submitted to**
**The Graduate School of Engineering and Science of**
**İzmir Institute of Technology**
**In Partial Fulfillment of the Requirements for the Degree of**

**MASTER OF SCIENCE**

**In Materials Science and Engineering**

**by**
**Remziye YILDIZ**

**June 2021**
**İZMİR**

# ACKNOWLEDGEMENTS

I would first like to thank my supervisor Assoc. Prof. Dr. Yaşar Akdoğan. The door to his office was always open whenever I ran into a trouble spot or had a question about my research or writing. He consistently allowed this thesis to be my own work, but steered me in the right the direction whenever he thought I needed it. Thanks to academic and personal guidance, his endless patience and support throughout this work. It was honour to study with him.

My special thanks to Prof. Dr. Mustafa Emrullahoğlu for permission to enable using his laboratory facilities and his support on my thesis.

I would like to thank the TUBITAK (118Z552) for supporting me during the project.

I would also like to thank sincerely the two of the co-authors of our paper; Prof. Dr. Hasan Şahin and Sercan Özen, who contributed to our paper substantially and gave an important perspective.

My special thanks to Melih Kuş who helped me to read and to take the NMR datas.

Also I would like to thank Prof. Dr. Hasan Şahin, and Asst. Prof. Dr. Muhammed Üçüncü for participating as a committee member and reviewing my work.

The biggest thanks are to my dear mother Beyaz Yıldız, my father Abdulbaki Yıldız, my sisters Hülya, Burçin, Özlem and my brothers Mehmet and Ramazan, who are always with me unconditionally, lift me whenever I fall, are behind me in every decision, who believe in my efforts whatever I do and what will I do, and do their best to motivate me. I love them so much.

One of the most important thanks belongs to my dear friends Barış Yıldırım, Sümeyra Sözer, Tuğçe Özmen Egesoy, Begüm Demirkurt whom I shared the same laboratory throughout my Master's life. We became lifelong friends who supported each other under all conditions. Finally, I would like to thank my boyfriend Eray Ceyhan deep from my hearth for being my morally and motivationally compass throughout years.

# ABSTRACT


## STUDYING DOPA ADHESION ON POLYSTYRENE UNDER WATER

Mussels wet adhesive performance has been arousing curiosity for a long time. It is found that 3,4-dihydroxyphenylalanine (DOPA) is responsible for adhesive properties of mussels. Despite a large body of research characterizing the interactions DOPA with hydrophilic surfaces, relatively few works have addressed the mechanism of interactions with hydrophobic surfaces. The benzene ring of DOPA is the main attributor to the adhesion on hydrophobic polystyrene (PS) surface. However, here we showed that two hydroxyl groups of catechol have also effects on wet adhesion. We studied wet adhesive properties of DOPA, tyrosine and phenylalanine functionalized PEG polymers, PEG-(N-Boc-L-DOPA)$_4$, PEG-(N-Boc-L-Tyrosine)$_4$, PEG-(N-Boc-L-Phenylalanine)$_4$, on spin labeled PS nanobeads (SL-PS) by electron paramagnetic resonance (EPR) spectroscopy. Surface coverage ratio of SL-PS upon additions of PEG-(N-Boc-L-DOPA)$_4$, PEG-(N-Boc-L-Tyrosine)$_4$ and PEG-(N-Boc-L-Phenylalanine)$_4$ showed that SL-PS was covered with 70%, 50% and 0%, respectively. This showed that spontaneous wet adhesion on PS increases with the number of amino acids hydroxyl groups. This is also supported with the density functional theory (DFT) energy calculations and ab-initio molecular dynamics (AIMD) simulations. In water, interactions between water molecules and hydroxyl groups on the catechol induce catechol adhesion via π-π stacking between the catechol and double styrene rings which were already tilted out with water.

# ÖZET

## DOPA'NIN SU İÇERİSİNDE POLİSTİRENE YAPIŞMA ÇALIŞMASI

Midyenin ıslak yapışkanlık performansı uzun zamandır merak uyandırmaktadır. Midyelerin yapışkan özelliklerinden 3,4-dihidroksifenilalaninin (DOPA) sorumlu olduğu bulunmuştur. DOPA'nın hidrofilik yüzeylerle etkileşimlerini karakterize eden araştırmalar bulunmasına rağmen, nispeten az sayıda çalışma hidrofobik yüzeylerle olan etkileşim mekanizmasına değinmiştir. DOPA'nın benzen halkası, hidrofobik polistiren (PS) yüzey üzerindeki yapışmaya ana katkı sağlar. Bununla birlikte, burada iki hidroksil katekol grubunun da ıslak yapışma üzerinde etkileri olduğunu gösterdik. Elektron paramanyetik rezonans (EPR) spektroskopisi ile spin etiketli PS nano tanecik (SL-PS) üzerinde DOPA, tirozin ve fenilalanin ile işlevselleştirilmiş PEG polimerlerinin, PEG-(N-Boc-L-DOPA)$_4$, PEG-(N-Boc-L-Tirozin)$_4$, PEG-(N-Boc-L-Fenilalanin)$_4$, ıslak yapışkan özelliklerini inceledik. PEG-(N-Boc-L-DOPA)$_4$, PEG-(N-Boc-L-Tirozin)$_4$ ve PEG-(N-Boc-L-Fenilalanin)$_4$ eklenmesi ile SL-PS'nin yüzey kaplanma oranı sırasıyla %70, %50 ve %0 olarak bulunmuştur. Bu, PS üzerindeki kendiliğinden gerçekleşen ıslak yapışmanın amino asit hidroksil gruplarının sayısı ile arttığını göstermiştir. Elde edilen sonuçlar yoğunluk fonksiyonel teorisi (DFT) enerji hesaplamaları ve ab-initio moleküler dinamik (AIMD) simülasyonları ile de desteklenmiştir. Su içerisinde, su molekülleri ve katekol üzerindeki hidroksil grupları arasındaki etkileşimler, katekol ve halihazırda suyla eğilmiş olan çift stiren halkaları arasındaki π-π yığılması yoluyla katekol yapışmasına neden olmaktadır.

# TABLE OF CONTENTS

# LIST OF FIGURES

**Figure** **Page**

**Figure** **Page**

**Figure** **Page**

# LIST OF TABLES

**Table** **Page**

# LIST OF ABBREVIATIONS

| | |
|---|---|
| DOPA | L-3,4-dihydroxyphenylalanine |
| Mfps | Mussel Foot Proteins |
| TFA | Trifluoroacetic Acid |
| Trp | Tryptophane |
| Tyr | Tyrosine |
| Phe | Phenylalanine |
| 5HTP | 5 Hydroxy Tryptophan |
| NaCl | Sodium Chloride |
| NaHCO | Sodium Bi-carbonate |
| Na2SO4 | Sodium Sulfate |
| THF | Tetrahydrofuran |
| DCM | Dichloromethane |
| DMF | N,N-dimethlyformamide |
| DMSO | Dimethyl Sulfoxide |
| SLPS | Spin Labeled Polystyrene Nanoparticle |
| Et3N | Triethylamine |
| MES | 2-(*N*-morpholino)ethanesulfonic acid |
| PEG | Polyethylene glycol |
| SFA | Surface Force Apparatus |
| Boc | di-tert-butyl-dicarbonate |
| EPR | Electron Paramagnetic Resonance |
| NMR | Nuclear Magnetic Resonance |
| UV-Vis | Ultraviolet-visible7 |
| HBTU | 2-(1H-benzotriazol-1-yl)-1,1,3,3-tetramethyluroniuhexafluorophosphate |
| HOBT | 1-hydroxybenzotriol |

# CHAPTER 1

# INTRODUCTION

## 1.1. Mussel Foot Proteins (Mfps)

Mussels can adhere to different types of surfaces such as rocks, piers, ships, etc. in the water due to their adhesive mussel foot proteins (Mfps) (Waite, 2017). Mfps secreted by mussels form strong adhesive plaques that can attach to wet surfaces (Dalsin et al., 2003). Mussels adhere to a sample surface with a byssus formed by a bunch of threads and plaques at the ends of the threads (Figure 1.1).

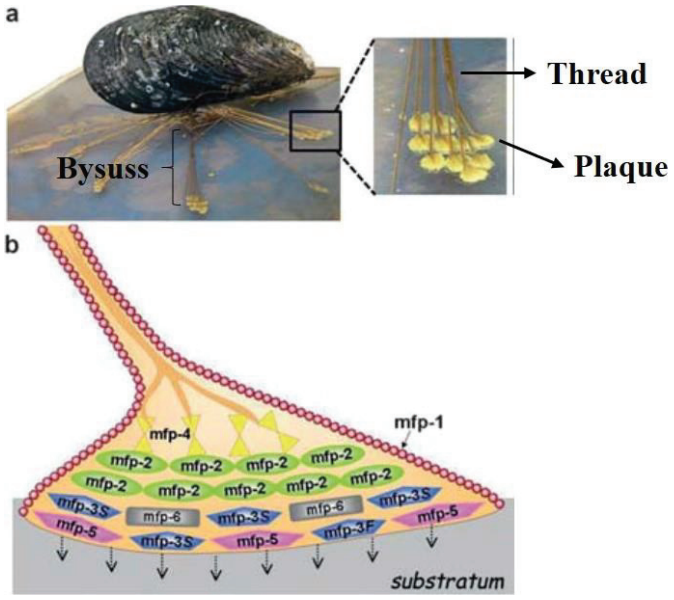


Figure 1. 1. (a) A mussel (Mytilus californianus) attached to a surface by a byssus formed by a bunch of adhesive-tipped threads. (b) Schematic representation in (a) extended of one of the adhesive plaques to indicate the approximate location of known Mfps (Source Akdogan et al., 2014).

The presence of L-3,4-dihydroxyphenylalanine (L-DOPA), an amino acid that is believed to be responsible for both the crosslinking and adhesion characteristics of Mfps,

is one of the unique characteristics of Mfps (Table 1.1). DOPA's catechol form is believed to be responsible for substrate adhesion (Zeng et al., 2000).

| Protein | Mass, kDa | pI | DOPA, mol% | Location |
|---|---|---|---|---|
| mfp-1 | 108 | 10 | 10–15 | Cuticle |
| mfp-2 | 45 | 9 | 5 | Plaque |
| mfp-3 | 5–7 | 8–10 | 10–20 | Plaque |
| mfp-4 | 90 | 10.5 | 2 | Plaque |
| mfp-5 | 9 | 9–10 | 30 | Plaque |
| mfp-6 | 11 | 10 | 2 | Plaque |
| preColD | 240 | 9 | <1 | Thread, plaque |
| preColNG | 240 | 9 | <1 | Thread, plaque |

Table 1. 1. Comparison of the DOPA-containing proteins in the adhesive plaques and threads of Mytilus species (Source: Lin et al., 2006)

The abundance of the catecholic amino acid, DOPA, in their protein sequences is one of the special features of Mfps. It is believed that the presence of catechol plays a dual role of interfacial binding and the solidification of the adhesive proteins. DOPA is formed by the conversion of tyrosine amino acid as a result of an enzymatic reaction using the tyrosinase enzyme (Figure 1.2).

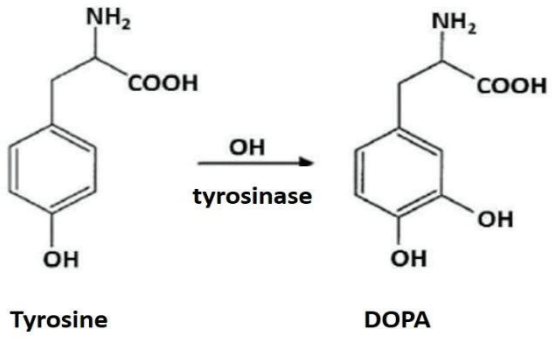


Figure 1. 2. Formation of a DOPA amino acid from tyrosine.

DOPA content varies between 0.1% and 30 moles of Mfp according to their location and function (Lee et al., 2011). When the sticky plaques of mussel were examined, the content of DOPA was higher in the proteins (Mfp-3: 20 mol% and Mfp-5: 30 mol% DOPA) in the part of contacting the surface (Lee et al., 2011). It has been shown that catechol moiety of DOPA is responsible for both adhesive and cohesive properties of mussels (Yang et al., 2016 and Gao et al., 2018). A benzene ring and two neighboring hydroxyl groups provide DOPA to interact with different types of surfaces via different types of interactions, ranging from weak dispersion forces to covalent bonds (Zhang et al., 2017). Several interaction mechanisms of DOPA with different surfaces have been reported, including hydrogen bonding, hydrophobic interactions, electrostatic interactions, π-π stacking, cation-π interactions and metal-complexation (Lu et al., 2013). DOPA has a strong affinity for hydrophilic surfaces, bidentate hydrogen bonding by DOPA is the main contributor to DOPA adhesion to mica and silica (Lu et al., 2013).

In the literature, the adhesion of Mfp's obtained from mussels to different surfaces has been studied (Waite et al., 2017). However, obtaining Mfp from mussels takes place as a result of a very laborious process. Only 1 g of Mfp-1 protein can be obtained from approximately 10,000 Medulis mussels (Hwang et al., 2007). Also, obtaining recombinant Mfp's is very complex and costly. Therefore, DOPA attached adhesive polymers have been studied instead of Mfps (Forooshani and Lee, 2017). Lee et al. obtained DOPA attached linear and branched poly (ethylene glycol) (PEG) polymers (Figure 1.3) (Lee et al., 2011).

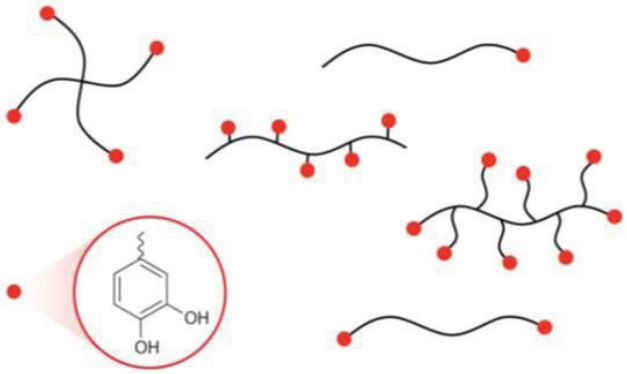


Figure 1. 3. Schematic diagram of mussel adhesive protein mimetic polymer systems. The red circles represent DOPA or a DOPA catechol mimic that is

covalently bound to polymer chain ends or as polymerizable catechol monomer side chains. (Source: Lee et al., 2011)

Conjugating a polymer end group with DOPA is the main approach in synthesizing these materials. There are different types of polymers backbones like polyethylene glycol (PEG) (Eberle et al., 2000), polymethyl methacrylate (Güvendiren et al., 2008), polysiloxane (Heo et al., 2012), poly(acrylic acid) (Laulicht et al., 2012 and Wang et al., 2008) etc., with different polymer conformations. The most abundant material in the literature is 4-arm PEG end functionalized with DOPA that is protected with di-tert-butyl dicarbonate (Boc) group (Figure 1.4).

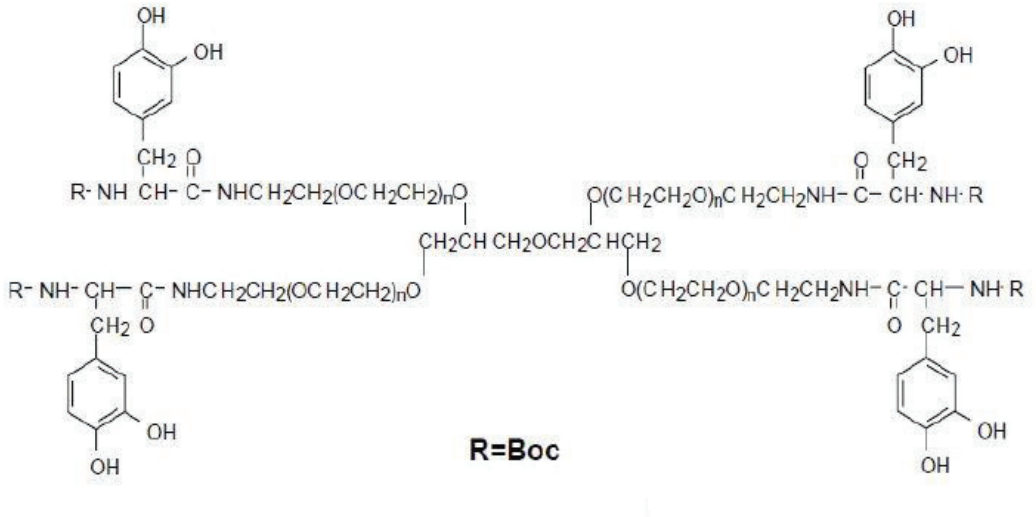


Figure 1. 4. Structure of PEG-(N-Boc-DOPA)$_4$
(Source: Eberle et al., 2000).

## 1.2. Tyrosine, Phenylalanine, Tryptophan, 5-Hydroxytryptophan Modified PEG Polymers

Similar to DOPA, other amino acids such as tyrosine (Tyr), phenylalanine (Phe), tryptophan (Trp) and 5-hydroxytryptophan have been studied to understand the adhesion mechanism of DOPA. The molecules of tyrosine (missing one of the two hydroxyl groups

of DOPA) and phenylalanine (missing hydroxyl groups of DOPA) were linked to the PEG polymer, and PEG-(N-Boc-L-Tyrosine)$_4$ and PEG-(N-Boc-L-Phenylalanine)$_4$ were obtained, respectively. Tryptophan and 5-hydroxytryptophan molecules (with a hydroxyl group attached to tryptophan) were also attached to PEG polymers, and PEG – (tryptophan)$_4$ and PEG – (5-hydroxytryptophan)$_4$, were obtained, respectively.

Understanding the mechanism of interaction of DOPA and related compounds, which are very useful for anchoring various molecules to surfaces, is critical for the design and creation of new materials, adhesives and coatings. Das and Reches looked at how different catechol moiety substitutions on the aromatic ring affected the amino acid residue's adhesion to the surface. They investigated the surface of titanium dioxide ($TiO_2$), since $TiO_2$ is the most suitable and promising semiconductor catalyst in heterogeneous photocatalysis among several significant metal oxides. By using single molecule force spectroscopy, they analyzed the rupture force of a DOPA molecule and other related single molecules to a $TiO_2$ surface. The used amino acid residues were : (i) phenylalanine (Phe), which has no hydroxyl (–OH) group substituent on its benzene ring, (ii) tyrosine (Tyr), which has one –OH group substituent, and (iii) L-3,4-dihydroxyphenylalanine (DOPA), which has two consecutive –OH groups (catechol group), (iv) 6-hydroxy-L-DOPA (6-OH-DOPA) with three hydroxyl groups, and (iv) 6-nitro-L-DOPA (6-NO2-DOPA) with an electronwithdrawing $NO_2$ group as an aromatic substituent (Figure 1.5). They observed that higher number of OH groups increased the rupture force.

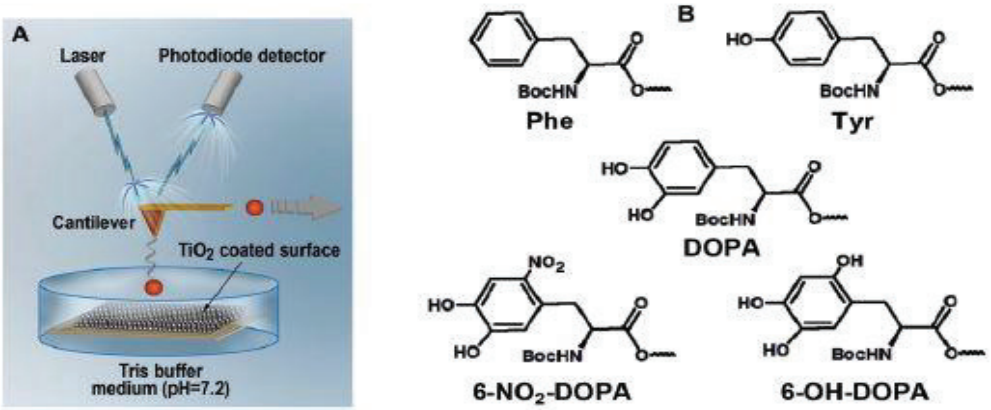


Figure 1. 5. (A) A schematic diagram of the SMFS experimental set-up for studying interactions between different amino acid moieties and the TiO2 surface. (B) Amino acid structure; the C-termini of the amino acid residues were coupled

to the AFM tip through polyethylene glycol (PEG, the flexible linker), and the N-termini were covered with Boc. (Source: Das and Reches, 2016).

## 1.3. Adhesion Measurements of DOPA to Different Wet Surfaces

The adhesion properties of synthetic polymers containing DOPA to different surfaces were measured by X-ray photoelectron spectroscopy (XPS) (Dalsin et al., 2003), sum frequency generation (SFG) spectroscopy (Leng et al., 2013), atomic force microscopy (AFM) (Lee et al., 2006 (b)), surface force apparatus (SFA) (Yu et al., 2011 (a)), lap shear technique (Matos-Perez et al., 2012). Figure 1.6 shows some of these techniques, e.g. AFM, SFA, and lap shear technique. In these techniques the polymers were adhered to selected surfaces by applying external forces and after that the adhesive strength during the separation of the surfaces was determined.

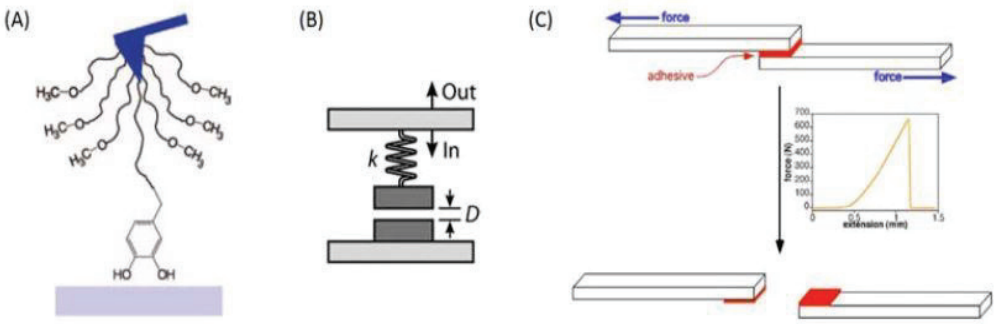


Figure 1. 6. Methods used in literature to calculate the adhesion properties of polymers modified by synthetic DOPA. (A) Atomic Force Microscope, (AFM) (Source: Lee et al., 2006). (B) The surface force apparatus, (SFA). (Source: 2011 by Yu et al.). (C) Lap shear technique (Source: Matos-Perez et al., 2012).

For example, it has been shown by SFG spectroscopy that poly (3,4-dihydroxy styrene-costyrene), which is inspired by proteins containing DOPA, can adhere to polystyrene and polyallylamine surfaces without and after crosslinking (Leng et al.,

2013). It bonds to hydrophobic polystyrene surface with π-π interaction, and to hydrophilic polyallylamine surface with hydrogen bonds (before crosslinking) and covalent bonds (after crosslinking, quinone). In addition, the adhesive strength of the produced polymer was measured using the lap shear technique, and it was shown that its adhesive strength is comparable with the commercial adhesives (Krazy glue, white glue, PVA, and Loctite) (Matos-Perez et al., 2012).

## 1.4. Electron Paramagnetic Resonance (EPR) Spectroscopy

Electron paramagnetic resonance (EPR) spectroscopy is a method to measure the paramagnetic properties of samples. EPR can be applied to the species with one or more unpaired electrons such as free radicals and transition metal compounds. Also it is useful for unstable paramagnetic compounds generated by electrochemical oxidation or reduction. If there is no paramagnetic group in the system, the material can be still studied with EPR spectroscopy by applying the spin probing and labeling methods (Kattnig et al., 2012; Kattnig et al., 2013; Göksel and Akdogan, 2019; Kırpat et al., 2017). Stable nitroxide radicals can be used for spin probing and labeling methods, non-covalently and covalently, respectively. Stable spin labels can be attached to the desired part of the material with covalent bonds so the surroundings of the label can be studied with EPR spectroscopy. Dynamic studies of the spin label from the analysis of the EPR spectrum can be performed in the picosecond-microsecond range (Hinderberger, 2011). If the rotational speed of the spin label is high, the spectrum consists of sharp signals, if the rotational speed of the spin label is slow, the spectrum consists of wide signals (Figure 1.7).

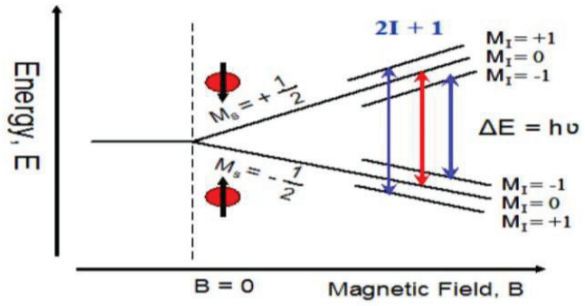


Figure 1. 7. Principle of EPR spectroscopy, energy vs magnetic field diagram (Source: Akdogan PhD thesis, 2009)

Electrons have a spin quantum number ($m_s = \pm 1/2$) and a magnetic moment. The electron's spin magnetic moment (μ) is aligned either parallel (-1/2) or antiparallel (+1/2) to the field in the presence of an external magnetic field (B), each having a particular energy (E). In other words, the two states are labeled by the projection of the electron spin, $m_s$, on the direction of the magnetic field, where $m_s = -1/2$ is parallel and $m_s = +1/2$ is antiparallel state. The lower energy state occurs when the magnetic moment of the electron is aligned with the magnetic field. The upper energy state occurs when the magnetic moment of the electron is aligned with the magnetic field.

$$\mathbf{E = \mu B} \qquad \mathbf{(1)}$$

The spin magnetic moment (μ) of free electron is given by;

$$\boldsymbol{\mu = (-1/2) g_e \beta} \qquad \mathbf{(2)}$$

where $g_e$ is the free electron Zeeman (correction) factor and β is the Bohr magneton**.** g-factor
is a signature for a material and it is generally the value of 2.0023 for free electron. Bohr magneton equals to $9.2700949 \times 10^{-24}$ $JT^{-1}$.

When the energy difference (ΔE) between spin energy levels is equal to the energy of the spin states separated by the applied magnetic field, the unpaired electron changes its spin state by receiving an appropriate microwave radiation at the specific microwave frequency ($\nu$). In other words, at a resonance condition external energy (microwave radiation) excites the unpaired electron from lower state to upper state.

$$\boldsymbol{\Delta E = h\nu = g_e \beta_e B} \qquad \mathbf{(3)}$$

Moreover, the magnetic moment produced by the orbital motion of the electron contributes to the total magnetic moment added to the free electron. Pure spin ground state is disrupted by this moment and it induces spin-orbit interaction. Depending on the axis system of a molecule called $g_x$, $g_y$ and $g_z$, there are three g values. These g values are identical to each other when the paramagnetic ion system has an isotropic form. In cases where distortions in the paramagnetic ion system induce anisotropy, $gx \neq gy \neq gz$ is obtained from anisotropic spectra.

Hyperfine splitting induced by the interaction between unpaired electron and the nuclear spin (I≠0) reveals the presence of neighbor nucleus around the unpaired electron. This interaction divides energy and the estimated number of splits by the equation of 2nI+1 (where n is the number of the effective nucleus and I is the number of the nuclear spin) (Akdogan, 2009).

Measurements of EPR absorbance are usually evaluated after taking the first spectrum derivative (Fig. 1.8). This technique is commonly used since the first derivative helps to observe small variations in the spectrum of absorbance.

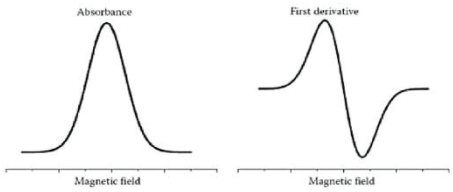


Figure 1. 8. Common absorbance spectra (left) and its first derivative (right) (Source: Talsi and Bryliakov, 2017).

EPR can analyze only paramagnetic materials, as discussed above. Addition of a spin label molecule to a diamagnetic material makes the sample EPR active (Tatlidil et al. 2015; Akdogan et al. 2016). 2,2,6,6-Tetramethylpiperidin-1-yl) oxyl (TEMPO) is one of the most widely used spin-label molecules. 4-carboxy-Tempo (Figure 1.9), for example, binds to the diamagnetic material via the carboxyl functional groups.

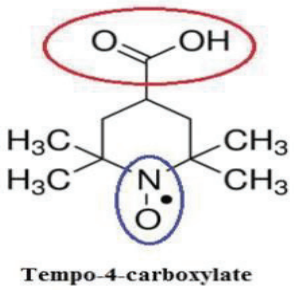


Figure 1. 9. Functional group (red circle) and radical group (blue circle) of 4-carboxy-Tempo. (Source: Kirpat MSc thesis, 2016)

Figure 1.10. shows the molecular structure of spin label 4-carboxy TEMPO and its EPR spectrum measured in liquid phase at room temperature. For TEMPO, because of the $^{14}N$ nucleus (n=1 and I=1), the EPR signal splits into 3 lines (number of splitting is 2nI+1) and has a g value about 2.0.

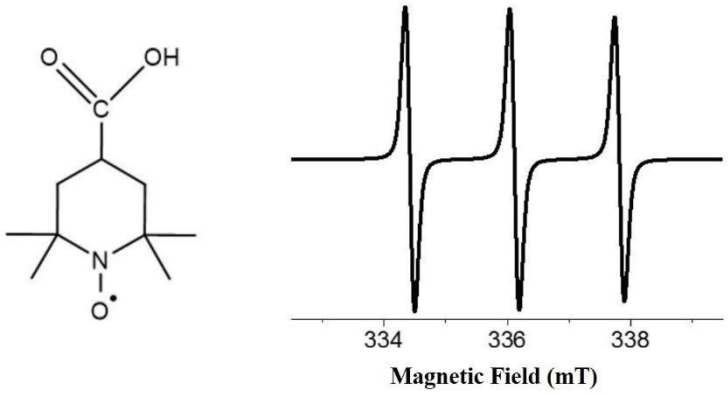


Figure 1. 10. Molecular structure of spin label 4-carboxy TEMPO (left) and its EPR spectrum measured in liquid phase at room temperature (right) (Source: Kırpat et al., 2017).

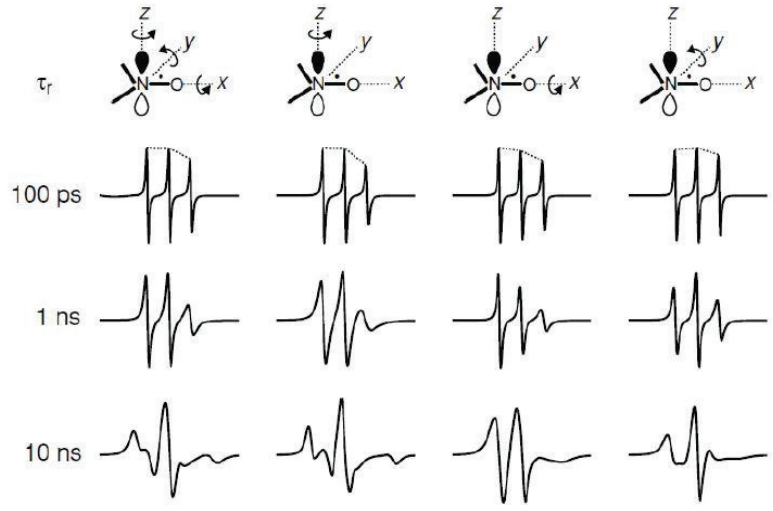


Figure 1. 11. EPR spectra of stable nitroxide radical when it has fast and slow motions with regards to spin axis in aqueous medium (Source: Hinderberger and Jeschke, 2008).

The variations in the nitroxide radical EPR spectra depending on the rotational correlation time are shown in Figure 1.11. Since the speed of rotational motion is directly influenced by its surrounding environment, distortions can be detected.

Akdogan et al. analyzed the variations of EPR spectra to investigate the adhesion of Mfps to spin labeled polystyrene and silica nanoparticles (Akdogan et al. 2014). Shortly, spin labels that have free motions yield sharper signals with shorter rotational correlation times, instead bound spin labels that have more restricted motions yield broader signals with longer rotational correlation times (Akdogan et al. 2014). The variation of the EPR spectrum was tested using spin labeled polystyrene (SL-PS) and spin labeled silica (SL-SiO2) nanobeads mixed with Mfps in solution (Fig. 1. 12).

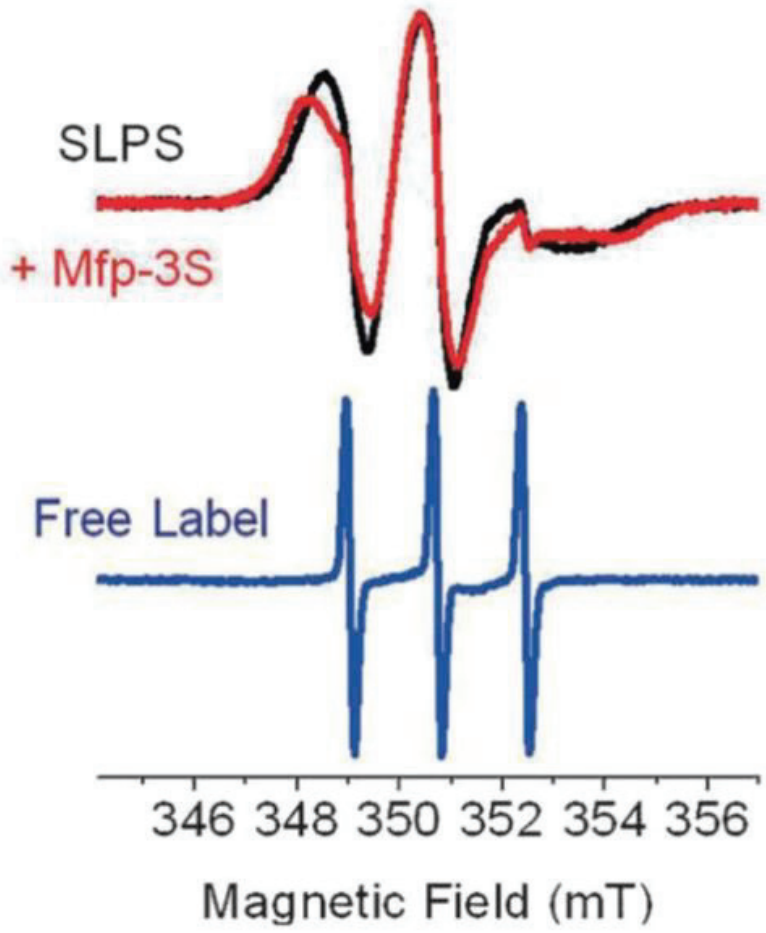


Figure 1. 12. Changing of the EPR signal after Mfp-3 adhesion on the surface of polystyrene (Source: Akdogan et al., 2014).

After binding on the polystyrene surface, the rotational speed of spin label molecules slows down significantly. In addition, Mfp-3 protein adhesion to the surface of polystyrene further impeded the rotational movement of the bound spin label. The rotational correlation time of free spin labels was found to be 20 ps and when applied to the polystyrene surface, it slowed down to 4.2 ns. In addition, Mfp-3 adhesion to SL-PS slowed down the spin label's rotational correlation time to 5.7 ns (Akdogan et al., 2014). When the spin label is attached to the surface of a nanoparticle, it can no longer move freely. The rotational speed of spin label depends on the rotational speed of the nanoparticle. Therefore, the EPR signals given by spin labels attached to the surface of the polystyrene nanoparticle are broader and the rotation correlation time is longer, around 4 ns. This shows that the surface of the polystyrene nanoparticle is covered with spin labels. Figure 1.13 shows the picture of the spin-labeled polystyrene nanoparticle and its EPR spectrum in liquid (Kırpat et al., 2017).

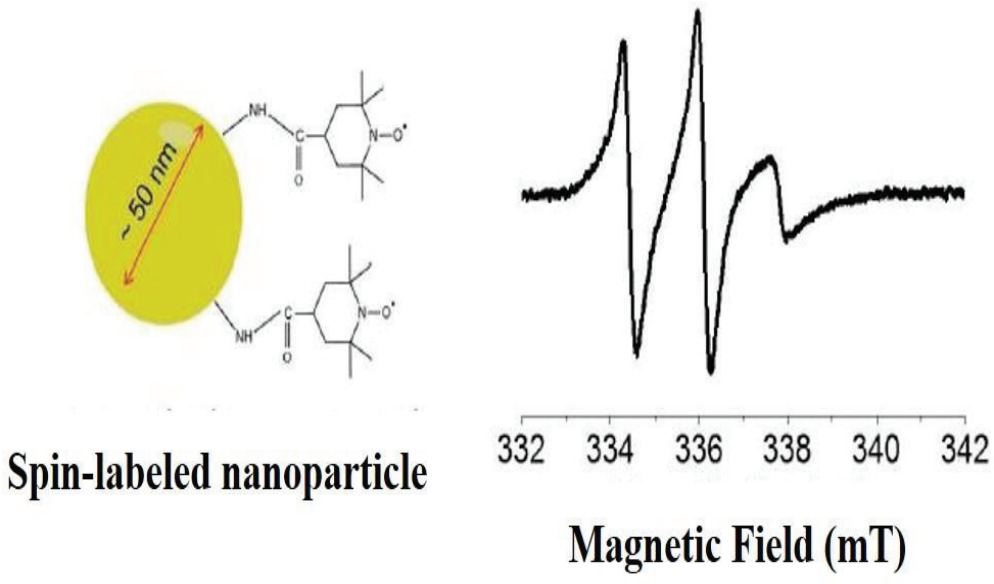


Figure 1. 13. Spin-labeled nanoparticle (left) and its EPR spectrum measured in aqueous solution (right) (Source: Kırpat et al., 2017).

## 1.5. Aim of the Thesis

The adhesion is carried out the catechol side of DOPA, but the role of hydroxyl (-OH) groups in hydrophobic surface adhesion is not well known. Changing the number of

hydroxyl groups on DOPA will enable us to better understand how hydroxyl (-OH) groups affect adhesion. Also, PEG modified with tryptophan in the previous study (Göksel et al., 2018) could not spontaneously adhere to polystyrene in spite of tryptophan is a hydrophobic amino acid. Because of these reasons, aim of the project is to understand reasons of adhesive ability of DOPA to polystyrene under water without applying force and to understand why tryptophan containing PEG polymer does not adhere to polystyrene. In order to understand the effect of DOPA hydroxyl groups on adhesion to the PS surface, tyrosine having a single hydroxyl group or phenylalanine without any hydroxyl group were attached to the 4-armed PEG polymers, and their adhesion properties were studied (Figure 1.14).

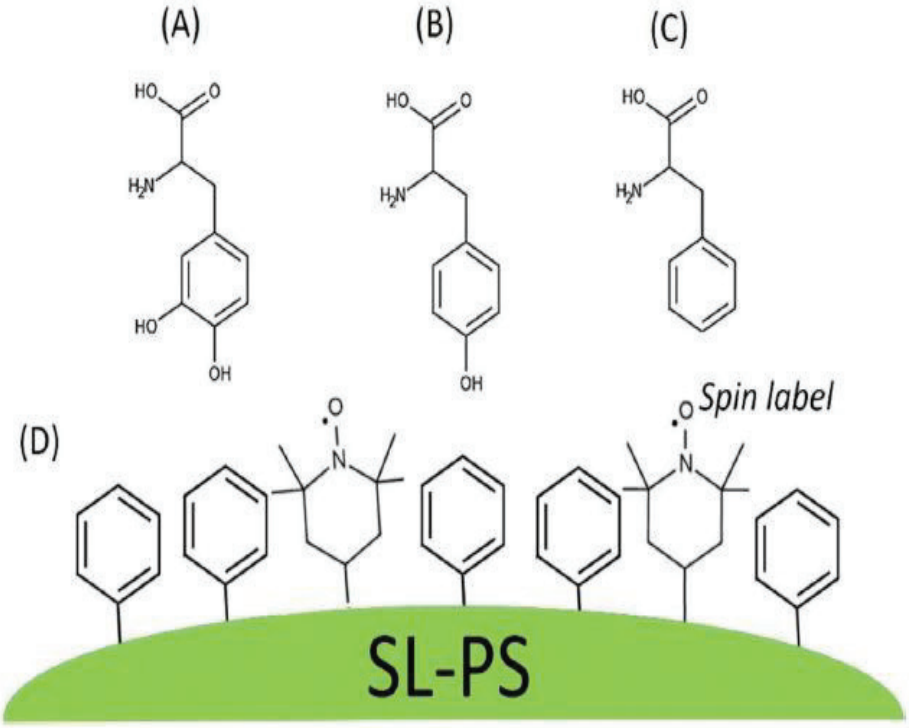


Figure 1. 14. Molecular structures of (A) L-DOPA, (B) L-Tyrosine, (C) L-Phenylalanine and (D) colloidal spin labeled polystyrene surface (SL-PS) (Source: Yildiz et al., 2019).

Tryptophan with no hydroxyl group and 5-hydroxytryptophan with a single hydroxyl group were attached to 4-armed PEG polymers and their adhesion properties

were analyzed to understand the effect of hydroxyl groups on adhesion to the PS surface (Figure 1.15).

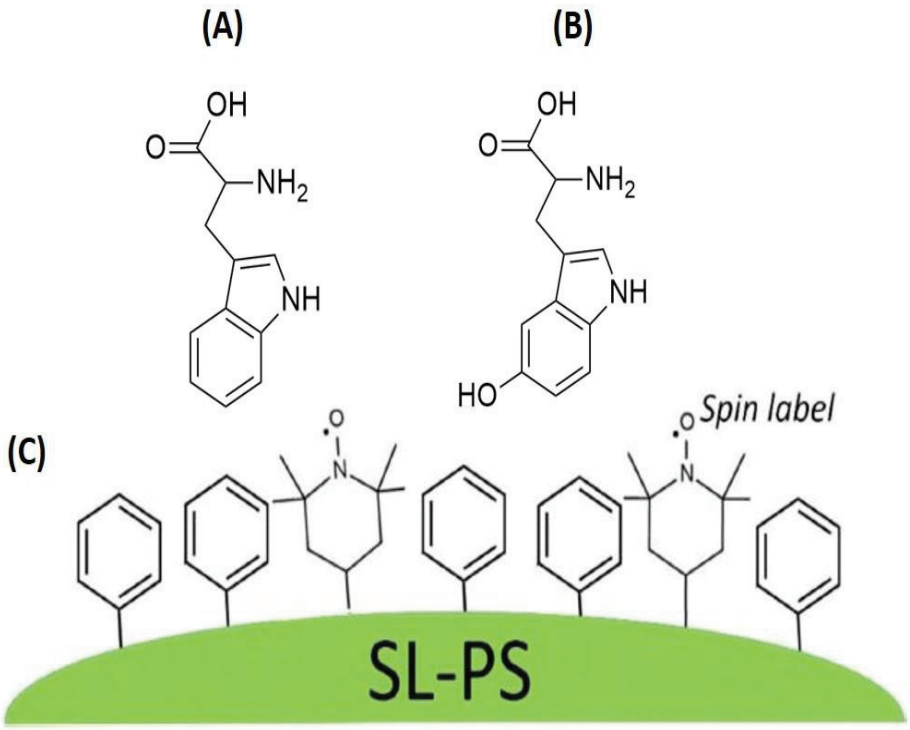


Figure 1. 15. Molecular structures of (A) L-Tryptophan, (B) L-5-Hydroxytryptophan and (C) colloidal spin labeled polystyrene surface (SL-PS).

# CHAPTER 2

# EXPERIMENTAL STUDY AND COMPUTATIONAL METHODOLOGY

## 2.1. General Methods

All reagents (Sigma Aldrich and Merck) were obtained from commercial suppliers and used without further purification. On a Varian VNMRJ 400 Nuclear Magnetic Resonance Spectrometer, the $^{1}H$ NMR was measured. The PerkinElmer UV/VIS Lambda 365 Spectrophotometer has been used to obtain UV absorption spectra. In quartz cuvettes, samples were placed in the instrument HI-8014 (HANNA) with a path length of 10.0 mm (2.0 mL volume). EPR spectra were measured using X-band Adani CMS 8400 EPR Spectrometer at room temperature.

## 2.2. Synthesis Section

### 2.2.1. Synthesis of N-Boc-L-DOPA

L-DOPA (78.85 mg, 0.4 mmol) and triethylamine (86 µL) were mixed in DCM:Dioxane (1:1) mixture (800 µL). Then the mixture cooled to 0 $^{o}$C (ice bath). Until all compounds were dissolved, di-tert-butyl decarbonate (98mg, 0.45 mmol) was dissolved in dioxane (400 µL) and added into the first mixture and was stirred at 0 $^{o}$C for 30 min (Figure 2. 1). After that the mixture was stirred at room temperature for 17 hours. After 17 hours, the mixture was extracted with ethyl acetate (50 mL) and the pH of the organic phase was adjusted to 1 by adding HCl (1N). Then the mixture was back extracted with ethyl acetate (50 mL) for 3 times. Organic phase was dried over $Na_2SO_4$ and also was evaporated to afford N-Boc-L-DOPA as a brown color which was used in the next step without any purification (84% yield) (Giorgioni et al., 2010, Kirpat et al., 2017 and Lee et al., 2002). $^{1}H$ NMR (400 MHz, DMSO-$d_6$) δ: 6.87 (d, 1H), 6.57 (s, 1H), 6.43 (d, 1H), 3.92 (br, s, 1H), 2.77-2.60 (m, 2H), 1.30 (s, 9H) (Figure A.1.).

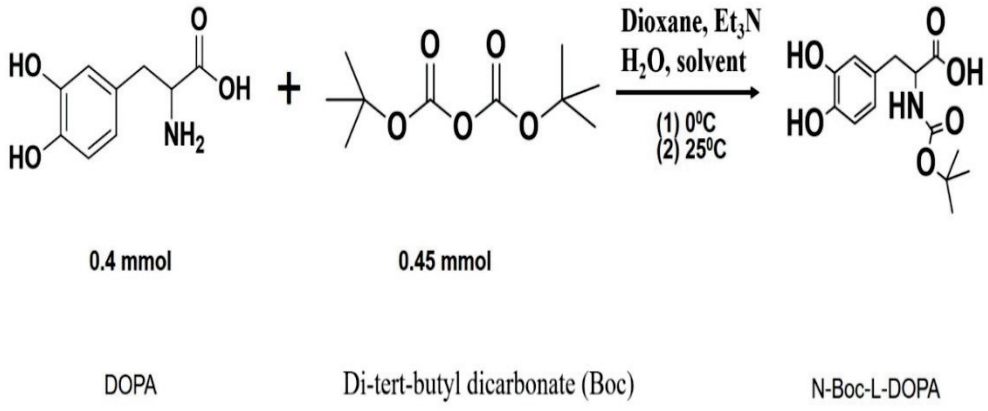


Figure 2. 1. Synthesis of N–Boc–L–DOPA

## 2.2.2. Synthesis of PEG-(N-Boc-L-DOPA)$_4$

PEG-$(NH_2)_4$ (10 kDa) (97 mg, $9.7x10^{-3}$ mmol), N-Boc-L-DOPA (23.9 mg, $80x10^{-3}$ mmol), 1-hydroxybenzotriazol (HOBT) (17.3 mg, 0.128 mmol), and triethylamine (17.6 µL) were mixed were dissolved in a mixture of DCM (460 µL) and DMF (460 µL) at 25 $^oC$. 2-(1H-benzotriazol-1-yl)-1,1,3,3-tetramethyluronium hexafluorophosphate (HBTU) (29.6 mg, 0.078 mmol), and DCM (460 µL) were added into the mixture and stirred at 25 $^oC$ under argon atmosphere for 5 hours. At the end of the experiment, ninhydrin test was applied to control the remained free primary amine left in the experiment setting. 2-3 drops of product was dissolved in DCM (1 mL) and 2-3 drops of ninhydrin solution was also added into the mixture. The mixture was stirred at 50 $^oC$ for 30 minutes, the test result was negative. The crude product was washed with a solution of saturated sodium chloride (50 mL), $NaHCO_3$ (5% w/mL), HCl (1 M) solution (50 mL), and distilled water (50 mL). The organic phase was dried over $Na_2SO_4$ and the product was precipitated in cold diethyl ether for 3 times to obtain PEG-(N-Boc-L-DOPA)$_4$ as a white solid (96% yield) (Lee et al., 2002). $^1$H NMR (400 MHz, DMSO-$d_6$) δ: 7.84 (s, 4H), 6.79-6.55 (m, 12H), 3.96 (br, s, 4H), 3.56-3.38 (m, 896H), 2.55–2.70 (m, 8H), 1.28 (s, 36H) (Figure A.2.).

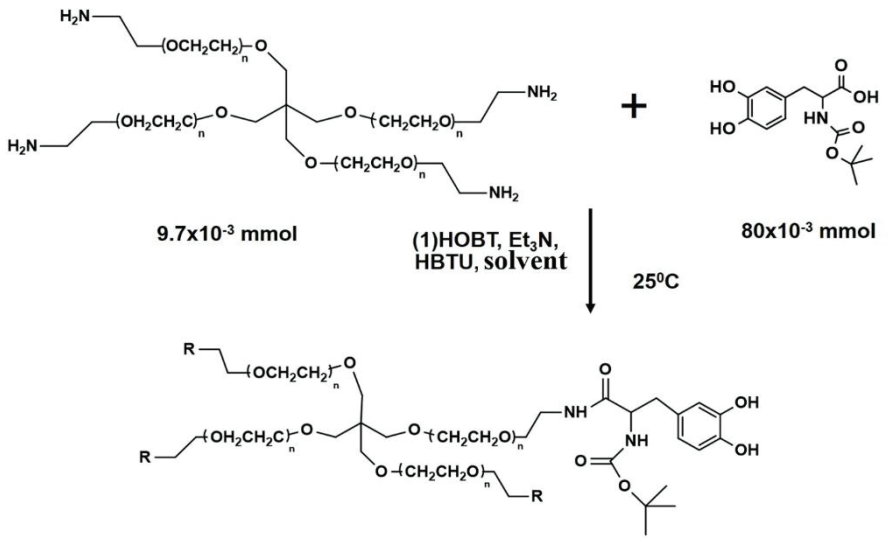


Figure 2. 2. Synthesis of PEG-(N–Boc–L–DOPA)$_4$

## 2.2.3. Synthesis of PEG-(N-Boc-L-Tyrosine)$_4$

PEG-($NH_2$)$_4$ (10 kDa) (97 mg, 9.7x10$^{-3}$ mmol), N-Boc-L-Tyrosine (23.9 mg, 80 x10$^{-3}$ mmol), 1-hydroxybenzotriazol (HOBT) (17.3 mg, 0.128 mmol), and triethylamine (17.6 µL) were mixed were dissolved in a mixture of DCM (460 µL) and DMF (460 µL) at 25 $^{o}$C. After all doing this steps, 2-(1H-benzotriazol-1-yl)-1,1,3,3-tetramethyluronium hexafluorophosphate (HBTU) (29.6 mg, 0.078 mmol), and DCM (460 µL) were added into the mixture and stirred at 25 $^{o}$C under argon atmosphere for 5 hours. At the end of the experiment, ninhydrin test was applied to control the remained free primary amine left in the experiment setting. 2-3 drops of product were dissolved in DCM (1 mL) and 2-3 drops of ninhydrin solution was also added into the mixture. The mixture was stirred at 50 $^{o}$C for 30 minutes, the test result was negative. The crude product was washed with a solution of saturated sodium chloride (50 mL), $NaHCO_3$ (5% w/mL), HCl (1 M) solution (50 mL), and distilled water (50 mL). The organic phase was dried over $Na_2SO_4$ and the product was precipitated in cold diethyl ether for 3 times to obtain PEG-(N-Boc-L-Tyrosine)$_4$ as a white solid (70% yield). $^1$H NMR (400 MHz, DMSO-$d_6$) δ: 7.84 (s, 4H), 7.05 (d, 8H), 6.59 (d, 8H), 4.00 (br, s, 4H), 3.47-3.38 (m, 896H), 2.75-2.57 (m, 8H), 1.27 (s, 36H) (Figure A.3.).

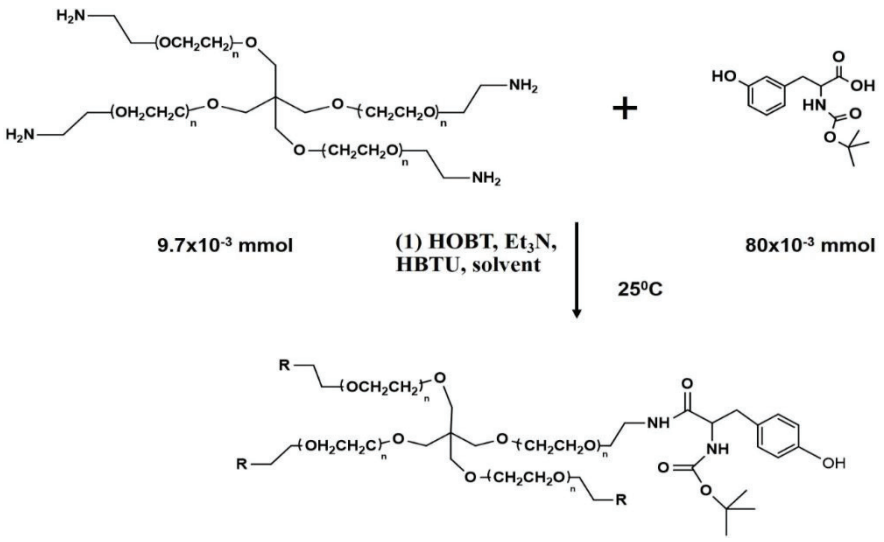


Figure 2. 3. Synthesis of PEG-(N–Boc–L–Tyrosine)$_4$

## 2.2.4. Synthesis of PEG-(N-Boc-L-Phenylalanine)$_4$

PEG-($NH_2$)$_4$ (10 kDa) (97 mg, 9.7x10$^{-3}$ mmol), N-Boc-L-Phenylalanine (23.9 mg, 80 x10$^{-3}$ mmol), 1-hydroxybenzotriazol (HOBT) (17.3 mg, 0.128 mmol), and triethylamine (17.6 µL) were mixed were dissolved in a mixture of DCM (460 µL) and DMF (460 µL) at 25 $^{o}$C. After all, doing this steps, 2-(1H-benzotriazol-1-yl)-1,1,3,3-tetramethyluronium hexafluorophosphate (HBTU) (29.6 mg, 0.078 mmol), and DCM (460 µL) were added into the mixture and stirred at 25 $^{o}$C under argon atmosphere for 5 hours. At the end of the experiment, ninhydrin test was applied to control the remained free primary amine left in the experiment setting. 2-3 drops of product were dissolved in DCM (1 mL) and 2-3 drops of ninhydrin solution was also added into the mixture. The mixture was stirred at 50 $^{o}$C for 30 minutes, the test result was negative. The crude product was washed with a solution of saturated sodium chloride (50 mL), $NaHCO_3$ (5% w/mL), HCl (1 M) solution (50 mL), and distilled water (50 mL). The organic phase was dried over $Na_2SO_4$ and the product was precipitated in cold diethyl ether for 3 times to obtain PEG-(N-Boc-L-Phenylalanine)$_4$ as a white solid (84% yield) (Lee et al., 2002). $^1$H NMR (400 MHz, DMSO-$d_6$) δ: 7.91 (s, 4H), 7.20 (m, 20H), 4.09 (br, s, 4H), 3.47-3.36 (m, 896H), 2.88-2.66 (m, 8H), 1.26 (s, 36H) (Figure A.4.).

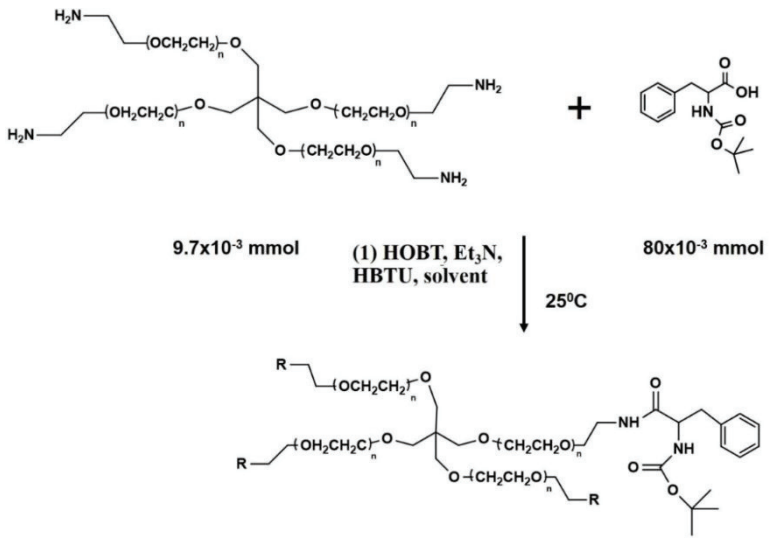


Figure 2. 4. Synthesis of PEG-(N–Boc–L–Phenylalanine)$_4$

## 2.2.5. Synthesis of PEG-(p-nitrophenyl carbonate)$_4$

PEG-(OH)$_4$ (10,000 g/mol) (214 mg, 21.4x10$^{-3}$ mmol) and p-nitrophenyl chloroformate (51.4 mg, 255x10$^{-3}$ mmol) were dissolved in dry DCM (3.5 mL), and stirred under argon atmosphere for 15 minutes. Then dry triethyl amine (25 μL) was added and the solution was stirred 24 hours a day at 25 ºC. At the end of the experiment TFA was added to the experiment until the experiment's color turned from yellow to colorless. After that the solvents was evaporated at rotary and the crude product precipitated in cold diethyl ether for 3 times to afford PEG-(p-nitrophenyl carbonate)4 as white powder (66% yield) (Mueller et al., 2011). $^1$H NMR (400 MHz, DMSO-$d_6$) δ: 8.30 (d, 8H), 7.53 (d, 8H), 4.39 (t, 8H), 3.53 (t, 8H), 3.46 (s, 896H) (Figure A.5.).

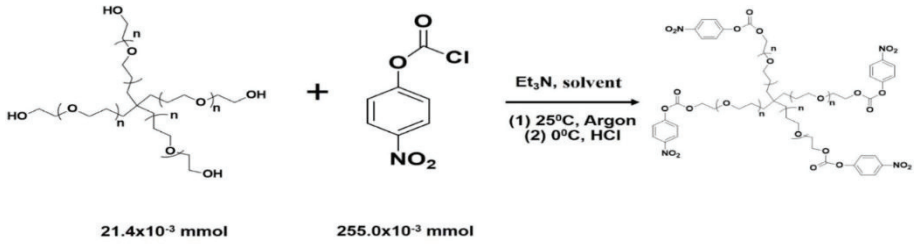


Figure 2. 5. Synthesis of PEG-(p-nitrophenyl carbonate)$_4$

## 2.2.6. Synthesis of PEG-(Tryptophan)$_4$

Tryptophane (227 mg, 1.12 mmol) and PEG-(p-nitrophenyl carbonate)$_4$ (300 mg, 27.9x10$^{-3}$ mmol) were mixed in dry DMSO (6 ml) and the mixture was stirred at 25 $^{o}$C for 5 hours. The experiment was then cooled to 0 $^{o}$C and the pH of the experiment was arranged to 3 by using HCl (2M) solution. After these steps the crude product was extracted for 8 times with chloroform, and dried over $Na_2SO_4$. After that solvents were evaporated at rotary and the crude product precipitated in cold diethyl ether for 3 times to afford PEG-(Trp)$_4$ as white powder (74% yield) (Mueller at al., 2011). $^1$H NMR (400 MHz, DMSO-$d_6$) δ: 10.95 (s, 4H), 7.52 (d, 4H), 7.32 (d, 4H), 7.18 (s, 4H), 7.05 (t, 4H), 6.96 (t, 4H), 3.86 (m, 8H), 3.47-3.27 (m, 896H), 3.04 (d, 8H) (Figure A.6.).

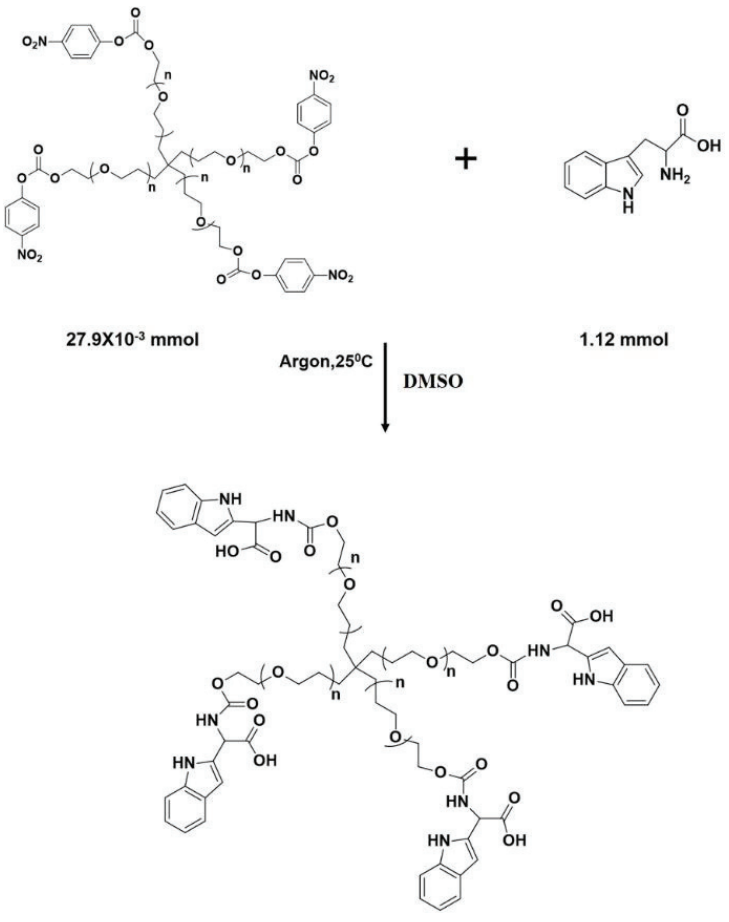


Figure 2. 6. Synthesis of PEG-(Tryptophan)$_4$

## 2.2.7. Synthesis of PEG-(5-HydroxyTryptophan)$_4$

In order to obtain PEG- (5-Hydroxytryptophan)$_4$, first PEG-(Paranitrophenylcarbonate)$_4$ was obtained from PEG- (OH)$_4$ and then PEG- (5 Hydroxytryptophan)$_4$ was obtained by using 5-Hydroxytryptophan with this product. 5-HydroxyTryptophane (227 mg, 1.12 mmol) and PEG-(p-nitrophenyl carbonate)$_4$ (300 mg, 27.9x10$^{-3}$ mmol) were mixed in dry DMSO (6 ml) and the mixture was stirred at 25 $^{o}$C for 5 hours. The experiment was then cooled to 0 $^{o}$C and the pH of the experiment was arranged to 3 by using HCl (2M) solution. After these steps the crude product was extracted for 8 times with chloroform, and dried over $Na_2SO_4$. After that solvents were evaporated at rotary and the crude product precipitated in cold diethyl ether for 3 times to afford PEG-(5-HydroxyTryptophan)$_4$ as white powder (88% yield) (Mueller at al., 2011). $^{1}$H NMR (400 MHz, DMSO-$d_6$) δ: 10.55 (s, 4H), 7.11 (s, 8H), 6.83 (s, 4H), 6.59 (d, 4H), 4.03 (m, 4H), 3.47 (m, 896H), 3.13 (d, 8H) (Figure A.7.).

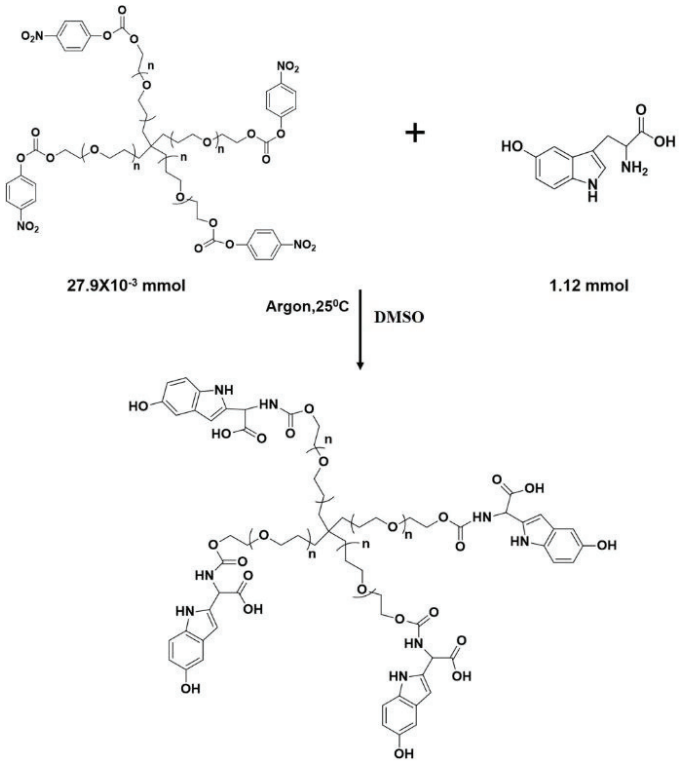


Figure 2. 7. Synthesis of PEG-(5-HydroxyTryptophan)$_4$.

## 2.2.8. Synthesis of Spin Labeled Polystyrene (SLPS)

Carbodiimide binding chemistry was used to label polystyrene nanoparticles with sizes around 50 nm with spin labels (4-carboxy Tempo). Polystyrene nanoparticle with amine groups on its surface was chosen as the starting material. Tempo-4-carboxylate (250 µL, 10 mM) in MES buffer (0.2 M) at pH 3.0 was combined with amine modified polystyrene bead (100 µL) in the presence of cross-linker, 1-ethyl-3-(3-dimethylaminopropyl) carbodiimide (EDC) (90 µL, 38 mM) for 24 hours at 29 $^{o}$C (Figure 2.8). EDC and free Tempo-4-carboxylate were washed out for several times with MES buffer, pH 3.0. (Akdoğan et al. 2014). Particle size was observed with dynamic light scattering (DLS) device and found as 52 nm.

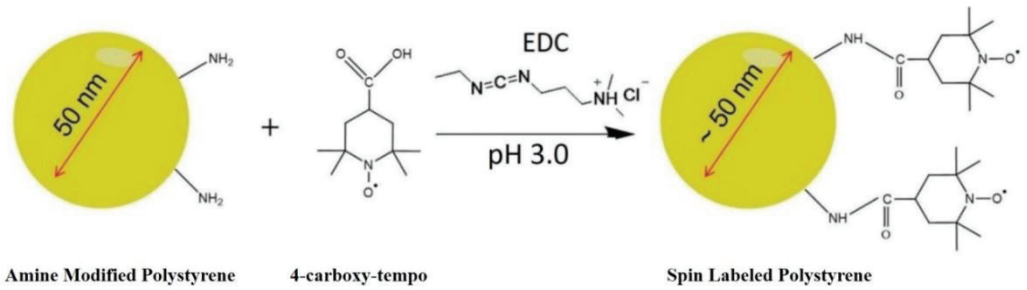


Figure 2. 8. Synthesis of Spin Labeled Polystyrene

## 2.2.9. Measurement of the adhesion of the obtained PEG polymers to spin-labeled PS nanoparticles by EPR spectroscopy

Adhesion tests were performed by preparing 180 mg/mL of functionalized PEG polymers in 0.2 M MES buffer solution at pH 3.0 and adding the same volume to MES buffer solution containing spin-labeled polystyrene. EPR measurements were taken by putting the mixture in quartz capillary tubes 5-10 minutes later. The simulations of the EPR spectra were simulated using a Matlab based Easypin 4.5.5 software package (Stoll et al., 2006). The EPR spectrum of spin-labeled polystyrene comes from the surface uncoated area (S1), while the signal from the surface coated with the addition of adhesive

polymers (S2) creates a new EPR spectrum. The resulting total spectrum was obtained by adding S1 and S2 in certain proportions $x_{(1)}$ and $x_{(2)}$.

$$\text{Spectrum obtained} = x_{(1)}S1 + x_{(2)}S2 \quad (4)$$

Surface coverage percentage is found by the following formula:

$$\% \text{ Coverage} = \text{Coated Area} / (\text{Coated Area} + \text{Uncovered Area}) \quad (5)$$

The covered area is obtained by multiplying $x_{(1)}$ by the area under the signal S1. The uncovered area is obtained by multiplying $x_{(2)}$ by the area under the S2 signal.

## 2.2.10. Computational Methodology

Interactions between styrene, water and catechol were investigated by performing density functional theory (DFT) based first-principle calculations as implemented in the Vienna ab initio simulation package (VASP) (Kresse et al., 1996). In addition to catechol, other similar structures such as phenol and benzene rings were analyzed in the styrene-water system. The Perdew-Burke-Ernzerhof (PBE) form of electron exchange and correlation and Becke-Johnson form of the van der waals correction were adopted (Perdew et al., 1996 and Grimme et al., 2011). For total energy calculations, all structures obtained from AIMD are fully relaxed until pressures in x, y, z directions are less than |1| kB. In the unit cell, the total force was reduced to a value less than $10^{-4}$ eV/A$^{o}$. For plane-wave basis set, kinetic energy cutoff was taken as 500 eV for all the calculations. The total energy difference between the sequential steps as a convergence criterion for ionic relaxations was set as $10^{-5}$ eV. In addition, the binding energies of structures, EB, were calculated using the formula;

$$EB = (E_{Molecule} + E_{Double\ Styrene} + E_{Double\ Water}) - E_{System} \quad (6)$$

Where $E_{Molecule}$ stands for the energy of an isolated molecule e.g. catechol, phenol or benzene, $E_{Double\ Styrene}$ is the energy of the total system of two styrene, $E_{Double\ Water}$ is the energy of two water molecule and $E_{System}$ is the calculated total energy of the system that includes styrene, water molecule and the molecule. In addition, we performed ab-initio molecular dynamic (AIMD) simulations to understand the interaction of styrene with catechol, phenol, and benzene both in non-aqueous and aqueous media. For the AIMD simulations, NVE ensemble is used. K-point sampling of the Brillouin is taken as 1 x 1 x 1 since the periodicity is not required. The temperature is increased from 50 to 450 up to 10 ps with a time step of 1 fs.

# CHAPTER 3

# RESULTS AND DISCUSSION

## 3.1. Characterization of PEG-(N-Boc-L-DOPA)$_4$, PEG-(N-Boc-L-Tyrosine)$_4$ and PEG-(N-Boc-L-Phenylalanine)$_4$

### 3.1.1. Nuclear Magnetic Resonance (NMR) Measurements

PEG-$(NH_2)_4$, (10 kDa) characterization of four-armed PEG polymers, individually functionalized with DOPA, tyrosine and phenylalanine, was performed by $^1$H NMR spectroscopy. Before the reaction with PEG-$(NH_2)_4$, the amino groups of the amino acids DOPA, tyrosine and phenylalanine were protected with the Boc group. Figure 3.1.1 starting material PEG-$(NH_2)_4$ and products, PEG-(N-Boc-L-DOPA)$_4$, PEG-(N-Boc-L-Tyrosine)$_4$, PEG-(N-Boc-L-Phenylalanine)$_4$ shows $^1$H NMR spectra.

The presence of signals around 7.0 ppm in the $^1$H NMR spectra of the functionalized products indicates that aromatic groups are attached to the PEG-$(NH_2)_4$ starting polymer. In addition, the presence of the signal at 1.40 ppm indicates the presence of methyl groups in the Boc group. From the area under the signals, the ratios of the proton numbers can be calculated and it can be found whether all four arms are bound by amino acids. The ratio of the proton signals in the methylene groups attached to the PEG polymer (3.62 - 3.69 ppm) to the area below the proton signals in the methyl groups in the Boc group (1.40 ppm) corresponds with the ratio of the proton numbers; 896: 36. This shows that N-Boc-L-DOPA N-Boc-L-Tyrosine and N-Boc-L-Phenylalanine are bound to all four arms of the PEG-$(NH_2)_4$ polymers.

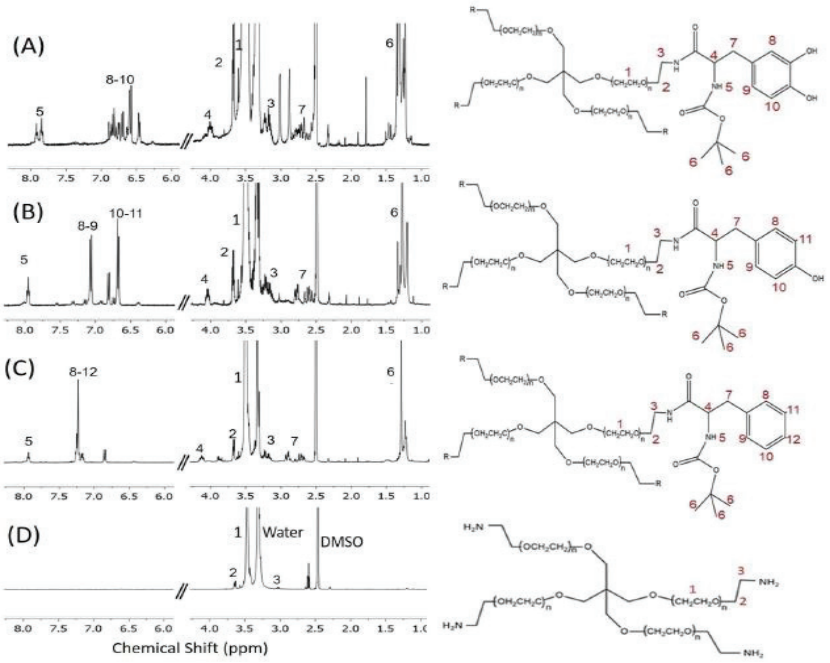


Figure 3. 1. 1. $^{1}$H NMR results and structures of (A) PEG-(N-Boc-L-DOPA)$_4$, (B) PEG-(N-Boc-L-Tyrosine)$_4$, (C) PEG-(N-Boc-L-Phenylalanine)$_4$ and (D) PEG-($NH_2$)$_4$ in deuterated DMSO.

## 3.1.2. Ultraviolet-Visible Spectroscopy (UV-Vis) Measurements

Bindings of N-Boc-L-DOPA, N-Boc-L-Tyrosine and N-Boc-L-Phenylalanine to PEG-($NH_2$)$_4$ were also observed by UV-Vis spectroscopy. UV-Vis spectra of 1.94 x $10^{-4}$ M N-Boc-L-DOPA, N-Boc-L-Tyrosine and N-Boc-L-Phenylalanine in MES buffer solution at pH 3.0 are shown in Figure 3.1.2. The signals obtained are due to π-π transitions in the aromatic ring (Antosiewicz et al., 2016). The maximum absorbance signal of N-Boc-L-DOPA was observed at 279 nm. In addition, the molar absorption coefficient was found to be $\varepsilon_{279}$ = 2242 $M^{-1}$ $cm^{-1}$. The maximum absorbance signal of N-Boc-L-Tyrosine was observed at 275 nm and the molar absorption coefficient has been found as $\varepsilon_{275}$ = 1340 $M^{-1}$ $cm^{-1}$. The spectrum of N-Boc-L-Phenylalanine is slightly wider (240-270 nm), but it gives a weaker signal. The maximum absorbance signal of N-Boc-L-Phenylalanine was observed at 257 nm and the molar absorption coefficient was calculated as $\varepsilon_{257}$ = 170 $M^{-1}$ $cm^{-1}$.

UV-Vis spectra of N-Boc-L-DOPA, N-Boc-L-Tyrosine and N-Boc-L-Phenylalanine and their UV-Vis spectra measured after binding to PEG-$(NH_2)_4$ are very similar. This indicates that these molecules are attached to the polymer (Figure 3.1.2). As expected, the starting material PEG-$(NH_2)_4$ has no UV-Vis absorbance signal. 0.485 x $10^{-4}$ M PEG-(N-Boc-L-DOPA)$_4$, PEG-(N-Boc-L-Tyrosine)$_4$ and PEG-(N-Boc-L-Phenylalanine)$_4$ showed absorbances at 279, 275 and 257 nm, respectively in pH 3.0 MES buffer solutions. In addition, since the absorbance intensities of these molecules (1.94 x $10^{-4}$ M) are the same before and after binding to the four arms of 0.485 x $10^{-4}$ M PEG-$(NH_2)_4$, there is a complete binding to PEG.

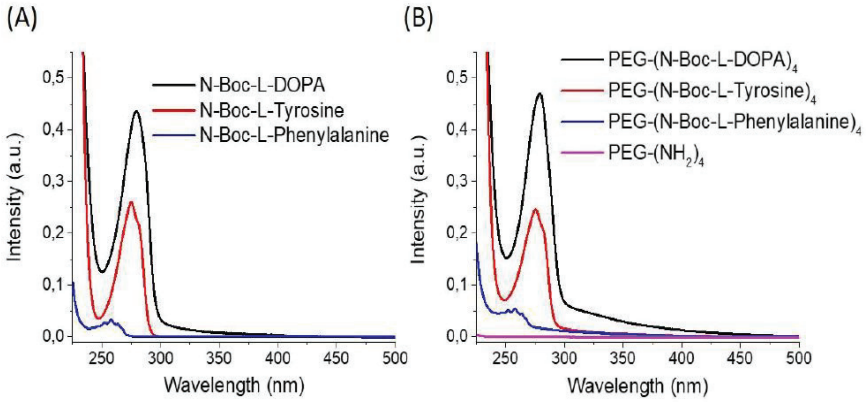


Figure 3. 1. 2. UV–Vis spectra of 1.94 x $10^{-4}$ M N-Boc-L-DOPA, N-Boc-L-Tyrosine and N-Boc-L-Phenylalanine before (A) and after (B) conjugation with 0.485 x $10^{-4}$ M PEG-$(NH_2)_4$. UV–Vis spectrum of the precursor PEG-$(NH_2)_4$ was also shown in (B). Samples were dissolved in 0.2 M MES buffer at pH 3.0.

## 3.2. Characterization of PEG-(Tryptophan)$_4$, and PEG-(5-HydroxyTryptophan)$_4$

### 3.2.1. Nuclear Magnetic Resonance (NMR) Measurements

Characterization of four-armed PEG polymers (10 kDa) functionalized separately with tryptophan and 5-hydroxytryptophan were performed by $^1$H NMR spectroscopy.

PEG-$(OH)_4$ was used as the starting polymer and then the more reactive PEG-(paranitrophenylcarbonate)$_4$ was obtained. Figure 3.2.1 shows the $^1$H NMR spectra of PEG-(paranitrophenylcarbonate)$_4$ and its products, PEG-(Tryptophan)$_4$ and PEG-(5-Hydroxytryptophan)$_4$.

New signals around 6.5 - 7.5 ppm in the $^1$H NMR spectra of the functionalized products indicate that aromatic groups are attached to the PEG-(paranitrophenylcarbonate)$_4$ polymer. According to NMR results, the ratio of PEG methylene protons (896) seen at 3.47 ppm to tryptophan and 5-hydroxytryptophan protons seen in the range of 6.50-7.45 ppm showed that tryptophan was bound to all four arms of the PEG-(paranitrophenylcarbonate)$_4$ polymer. In addition, the protons belong to the paranitrophenylcarbonate molecule at 8.30 and 7.55 ppm were not seen in the NMR result after the addition of tryptophan, which indicates that the paranitrophenylcarbonate molecule was removed from the four arms of the PEG.

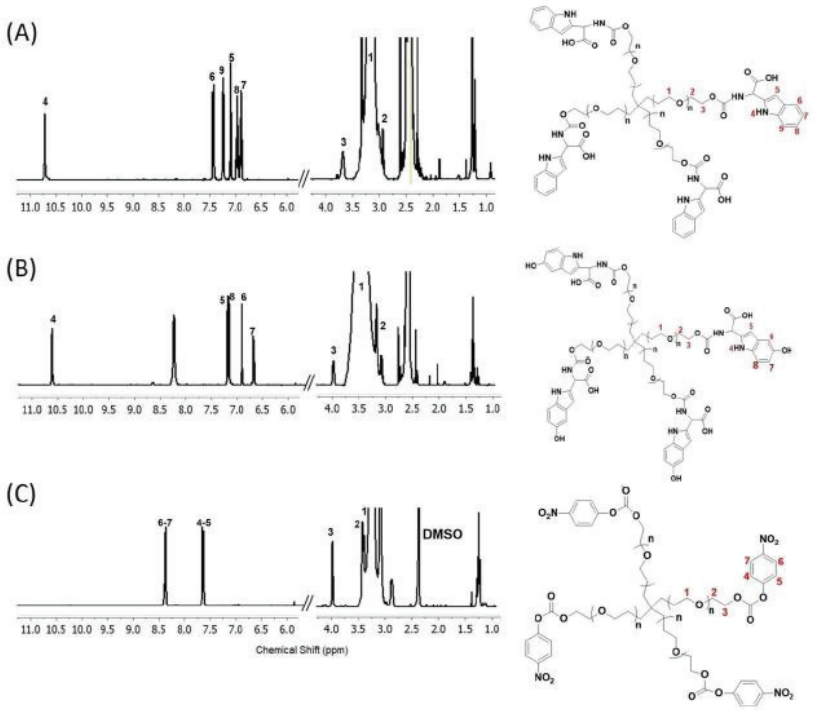


Figure 3. 2. 1. $^1$H NMR results and structures of (A) PEG-(Tryptophan)$_4$, (B) PEG-(5-HydroxyTryptophan)$_4$, and (C) PEG-(paranitrophenylcarbonate)$_4$ in deuterated DMSO.

### 3.2.2. Ultraviolet-Visible Spectroscopy (UV-Vis) Measurements

UV-Vis spectroscopy of tryptophan and 5-hydroxytryptophan bound PEG-(paranitrophenylcarbonate)$_4$ polymers were shown in Figure 3.2.2. The absorption signals obtained are due to π-π transitions in the aromatic rings of tryptophan and 5-hydroxytryptophan. The maximum absorbance signal of tryptophan was observed at 279 nm. In addition, the molar absorption coefficient was found to be $\varepsilon_{279} = 4023\ M^{-1}\ cm^{-1}$. Also, the maximum absorbance signal of 5-hydroxytryptophan was observed at 275 nm and the molar absorption coefficient was found to be $\varepsilon_{275} = 5402\ M^{-1}\ cm^{-1}$. The UV-Vis spectra of tryptophan and 5-hydroxytryptophan and their UV-Vis spectra measured after binding to PEG-(paranitrophenylcarbonate)$_4$ are very similar, indicating that these molecules are bound to the polymer (Figure 3.2.2.).

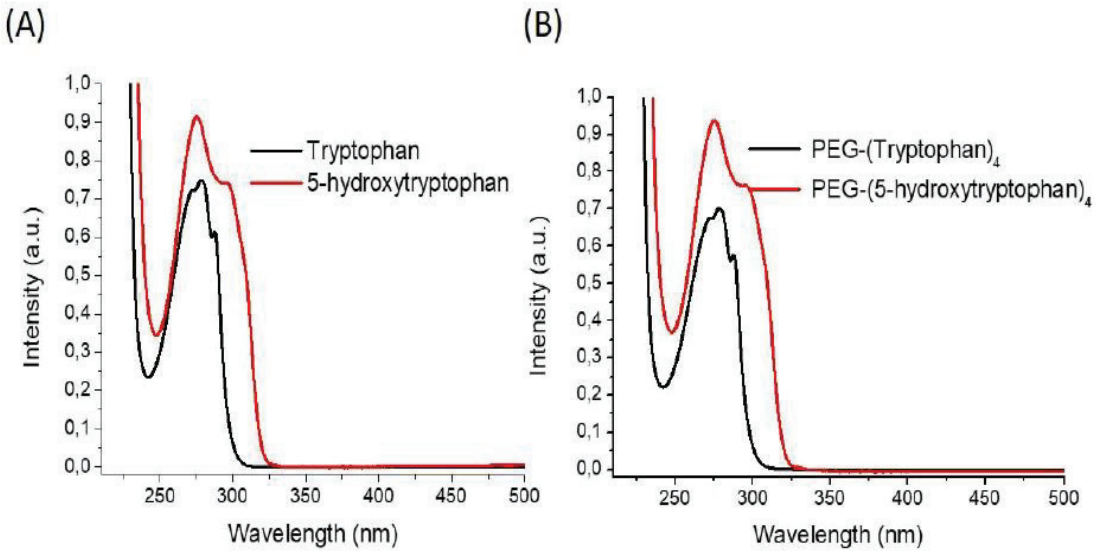


Figure 3. 2. 2. (A) UV-Vis spectra of 1.74 x $10^{-4}$ M tryptophan and 5-Hydroxytryptophan, and (B) UV-Vis spectra of tryptophan and 5-Hydroxytryptophan after binding to 0.435 x $10^{-4}$ M PEG-(paranitrophenylcarbonate)$_4$. Samples were prepared in 0.2 M MES buffer solution at pH 3.0.

## 3.3. Obtaining Spin-Labeled Polystyrene Nanoparticles

The EPR spectrum and simulation of the spin-labeled polystyrene (SL-PS) nanoparticles are shown in Figure 3.3. In addition, the EPR spectrum and simulation of 4-carboxy Tempo are also shown as a reference. Rotational movements of spin labels in liquid media affect the shape of the EPR signal. If the spin label can spin freely, the spectrum consists of sharp signals. By simulating the EPR spectrum of 4-carboxy Tempo, the correlation time of the rotational movement was found to be 20 ps. When the spin label is attached to the surface of a nanoparticle, it can no longer move freely and the rotational speed depends on the rotational speed of the nanoparticle. Therefore, the rotational correlation time of spin labels attached to the PS nanoparticle is prolonged, resulting in approximately 2 ns. This shows that the surfaces of PS nanoparticles are covered with spin labels.

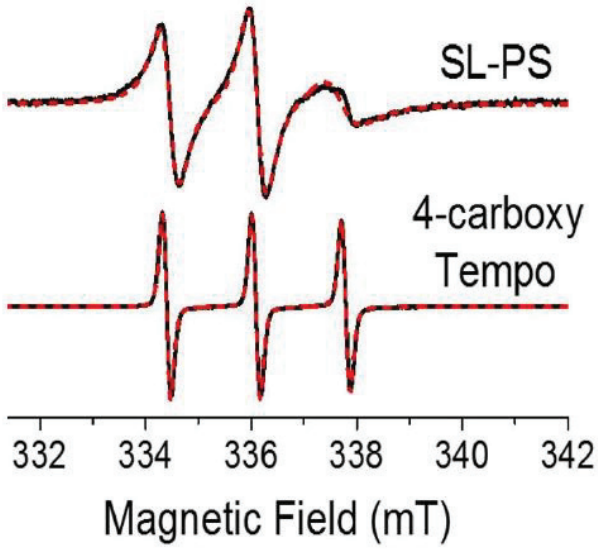


Figure 3. 3. EPR spectra (black) and simulations (red) of spin-labeled PS (SL-PS) nanoparticles as well as 4-carboxy Tempo. Measurements were taken in 0.2 M MES buffer (pH = 3.0).

## 3.4. Measuring the Adhesion of the Obtained PEG Polymers to Spin-Labeled Nanoparticles by EPR Spectroscopy

The adhesiveness of PEG polymers functionalized with tyrosine and phenylalanine was studied in order to understand the effect of hydroxyl groups in DOPA on the adhesion to hydrophobic polystyrene surface. Polymers dissolved in 0.2 M MES buffer solution (pH 3.0) were mixed with the same volume of 0.2 M MES (pH 3.0 to avoid DOPA oxidation (Cencer et al., 2014) buffer solution containing spin-labeled PS (SL-PS) nanoparticles, and adhesion experiments were performed by EPR spectroscopy. PEG polymers, whose final concentration in the mixture was set to be 90 mg/mL, were measured by EPR after mixing with SL-PS (Figure 3.4).

EPR spectrum of spin-labeled polystyrene did not change upon addition of PEG-(N-Boc-L-Phenylalanine)$_4$. This shows that PEG-(N-Boc-L-Phenylalanine)$_4$ does not adhere to SL-PS (Figure 3.4 (A)).

On the other hand, additions of PEG-(N-Boc-L-Tyrosine)$_4$ or PEG-(N-Boc-L-DOPA)$_4$, onthe SL-PS solutions changed the EPR spectra of SL-PS (Figure 3.4 (B) and (C)). A new type of spectrum was observed. Rotational correlation time of this new type of spectrum was found to be 10 ns. Therefore, there was a slowdown in the rotational speed of the spin labels. This is due to the adhesion of PEG-(N-Boc-L-Tyrosine)$_4$ and PEG-(N-Boc-L-DOPA)$_4$ to the PS surface and further restrictions on spin labels. As a result, the EPR spectrum consists of combining the EPR spectra of the non-coated (S1) and coated (S2) parts by polymers. In addition, the adhesiveness of PEG-($NH_2$)$_4$ was also tested. The EPR spectrum of SL-PS did not change upon addition of PEG-($NH_2$)$_4$ (Figure 3.4 (D)). This shows that PEG-($NH_2$)$_4$ could not adhere to PS surface.

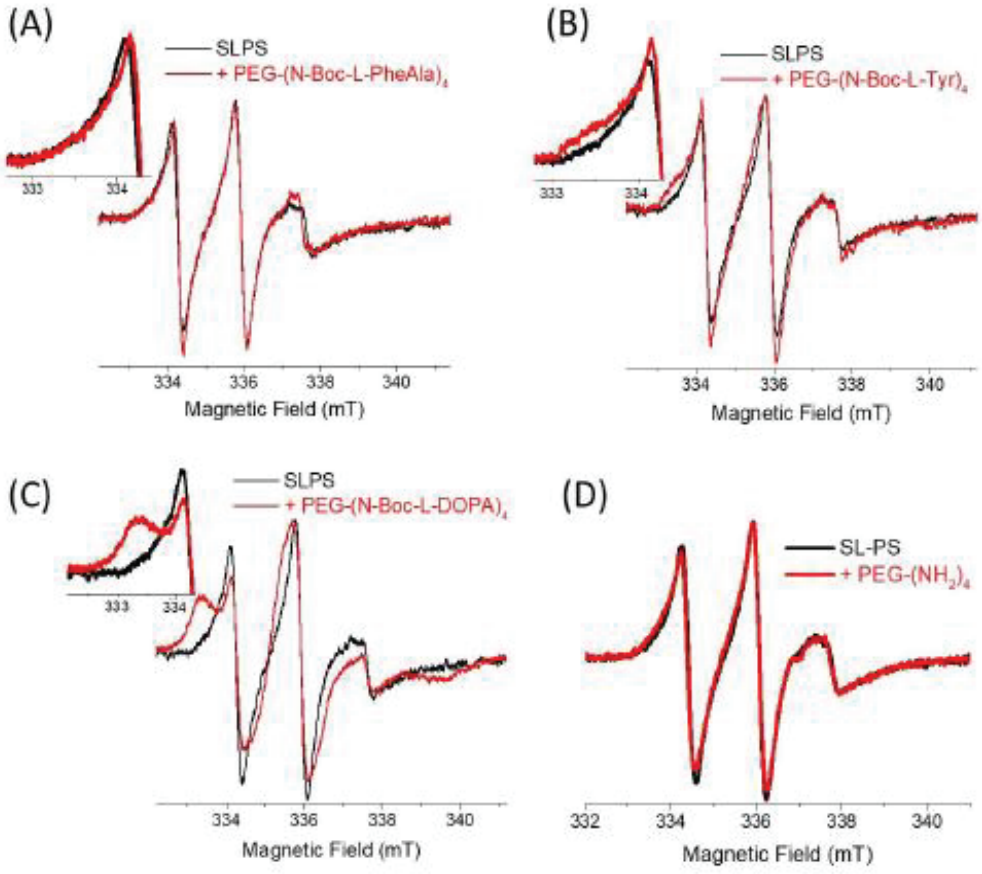


Figure 3. 4. EPR spectra of SL-PS before (black) and after addition of (A) PEG-(N-Boc-L-Phenylalanine)$_4$, (B) PEG-(N-Boc-L-Tyrosine)$_4$, (C) PEG-(N-Boc-L-DOPA)$_4$, and (D) PEG-($NH_2$)$_4$ (red).

EPR spectra were analyzed in order to measure the adhesion of PEG-(N-Boc-L-DOPA)$_4$ and PEG-(N-Boc-L-Tyrosine)$_4$ polymers to the polystyrene surface. The experimental result was obtained by finding the EPR signals coming from the uncoated (S1) and the coated (S2) parts of the surface by simulations (Figure 3.5). Proportional calculations can be made from the area under the signals. Areas under the EPR spectra of uncovered and covered SL on the PS were used to calculate the surface coverage (Part 2.2.9). Accordingly, after addition of PEG-(N-Boc-L-Tyrosine)$_4$ or PEG-(N-Boc-L-DOPA)$_4$ to SL-PS, the percentages of covered SL on PS were found 50 and 70%, respectively. These results showed that DOPA functionalized PEG polymer compared to tyrosine functionalized PEG polymer adhere to the PS surface more extensively. EPR results showed that the adhesion of four armed functionalized PEG polymers to PS

increases in the order: PEG-(N-Boc-L-DOPA)$_4$ > PEG-(N-Boc-L-Tyrosine)$_4$, and PEG-(N-Boc-L-Phenylalanine)$_4$ could not bind to the PS surface in the aqueous condition. This can be explained by the strong interactions between DOPA and styrene rings in the presence of water which are greater than the interactions between tyrosine and styrene rings. On the other hand, the interactions between phenylalanine and styrene rings must be very weak to achieve the wet adhesion.

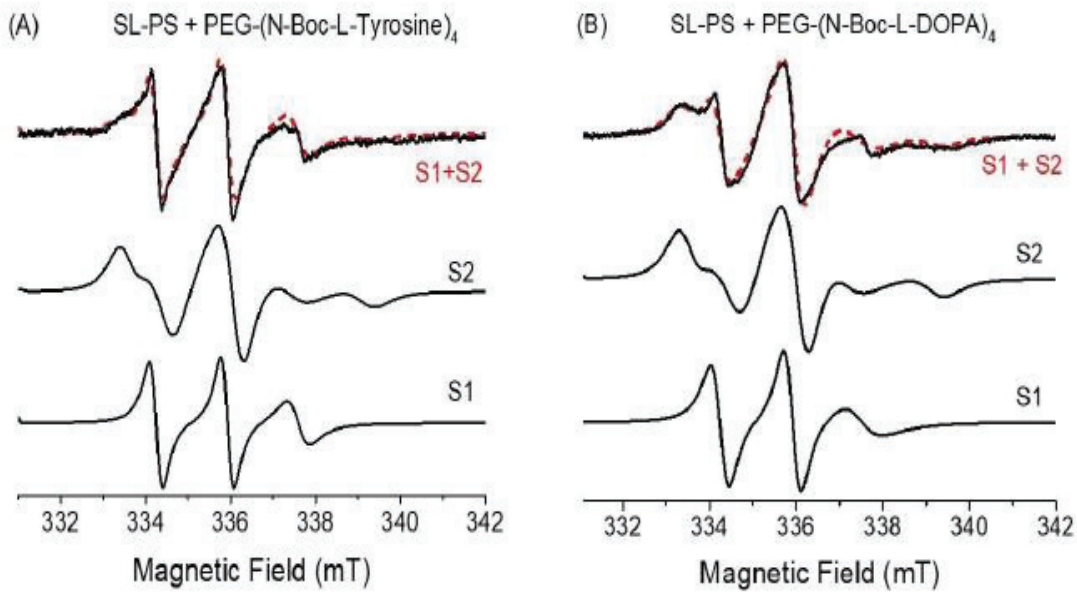


Figure 3. 5. Simulations of EPR spectra of uncovered (S1) and covered (S2) spin labels on PS with addition of (A) PEG-(N-Boc-L-Tyrosine)$_4$ or (B) PEG-(N-Boc-L-DOPA)$_4$. The sum of appropriate proportions of S1 and S2 yielded the experimental results obtained after addition of PEG-(N-Boc-L-Tyrosine)$_4$ or PEG-(N-Boc-L-DOPA)$_4$ with a final concentration 90 mg/mL (red, dashed lines).

Moreover, addition of PEG-(Tryptophan)$_4$ and PEG-(5-HydroxyTryptophan)$_4$ polymers separately to the SL-PS solution did not change the EPR spectrum of SL-PS significantly (Figure 3.6). This result showed that PEG-(Tryptophan)$_4$ and PEG-(5-Hydroxytryptophan)$_4$ polymers could not adhere to the surface of SL-PS in water.

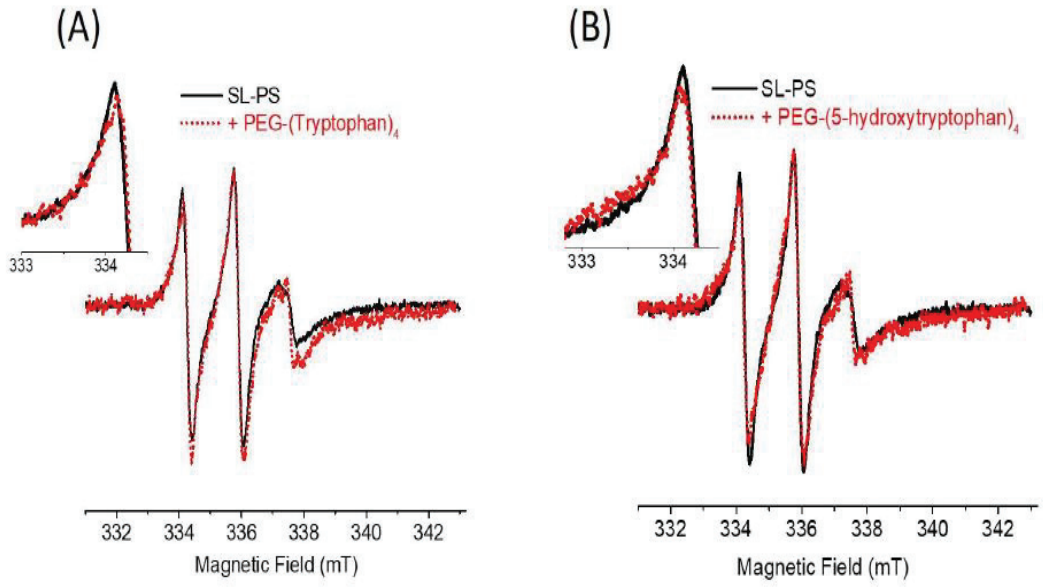


Figure 3. 6. EPR spectra of spin-labeled polystyrene (SL-PS) (black) and EPR spectra (red) after adding (A) PEG-(Tryptophan)$_4$ and (B) PEG-(5-Hydroxytryptophan)$_4$.

## 3.5. Binding energies and AIMD simulations of the styrene systems

In order to understand the reason of spontaneous wet adhesive ability of DOPA and

tyrosine but not phenylalanine functionalized PEG polymers to PS surface, total energy and molecular dynamics calculations were performed. Instead of DOPA, tyrosine and phenylalanine amino acids, the interactive sides of them such as catechol, phenol and benzene molecules, respectively, were used in the DFT calculations.

Although, the DOPA based adhesions on hydrophobic surfaces e.g. PS and CH3-terminated monolayers, have been studied experimentally (Leng et al., 2013, Danner et al., 2013 and Akdogan et al., 2014), only one theoretical study was performed up to now (Levine et al., 2016). Levine et al. applied a combination of surface forces apparatus (SFA) and molecular dynamics simulations on a DOPA-containing peptide which adheres strongly to CH3-terminated monolayers but adheres weakly to OH-terminated monolayers (Levine et al., 2016). In the literature, the most DOPA based adhesive both

experimental and/or theoretical studies have been investigated on hydrophilic and metal surfaces, e.g. silica, TiO2, mica, Cu (100), etc (Danner et al., 2013, Mian et al., 2010, and Chen et al., 2011).

While PS surface is considered hydrophobic, the benzene groups on the PS show hydrogen-bond accepting character. The estimated hydrogen bond strength between the aromatic ring of PS and water is higher than 110 meV which indicates the hydrophilic character of the aromatic moiety (Tretinnikov, 2000). Therefore, spontaneous adsorption of amino acids functionalized PEG polymers to PS surfaces could be affected by the pre-adsorbed water molecules on PS.

In Figure 3.7 (A), AIMD simulations revealed that two water molecules interact with two styrene molecules with a binding energy 485 meV due to the established hydrogen bonds between water-water and water-styrene, and also aromatic interactions between styrenes. After 2 ps, water molecules diffused between two styrene rings causing them tilting out (Figure 3.7 (A), 2 ps, side view). Addition of a catechol molecule to that system created new hydrogen bonds between two neighboring hydroxyl groups of catechol and water molecules. Furthermore, the conformation of styrene rings which were already tilted out enhanced the interaction between the catechol and styrene rings via π-π stacking in the presence of water (Figure 3.7 (B), 2 ps, side view). Therefore, the total binding energy of the catechol included system increased to 761 meV. Similar to the case of a catechol addition, a phenol molecule addition increased the total binding energy of system to 733 meV. Since phenol molecule has only one hydroxyl group, it forms less hydrogen bonds with water molecules compared to the number of hydrogen bonds formed between catechol and water. Also, AIMD simulations showed that styrene rings which were tilted out in water increased the phenol-styrene ring interactions via π-π stacking, too (Figure 3.7 (C), 2 ps, side view). On the other hand, addition of a benzene molecule to the system increased the total binding energy of system only to 562 meV from 485 meV. Since benzene does not have any hydroxyl groups, interaction between benzene and water is weaker than the interactions between catechol-water or tyrosine-water. In addition, AIMD simulations showed that styrene rings have a relatively closed structure (Figure 3.7 (D), 2 ps, side view) upon addition of a benzene molecule compared to the open structure of styrenes observed upon addition of catechol/phenol in water (Figure 3.7 (B, C), 2 ps, side views) which might be the reason of getting a less total binding energy.

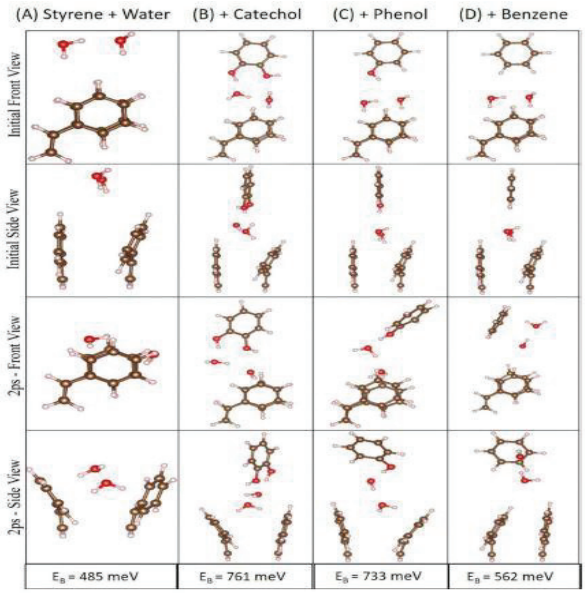


Figure 3. 7. AIMD simulations of the water including systems: initial and after 2 ps configurations with front and side views for the different systems composed of (A) two styrene and two water molecules, and after addition of (B) one catechol molecule, (C) one phenol molecule and (D) one benzene molecule. Total binding energies of the systems are shown under the views. Red, white and brown atoms represent oxygen, hydrogen and carbon atoms, respectively.

Without water systems, the conformations of styrene rings with respect to each other are also crucial for catechol, phenol and benzene binding. Figure 3.8 shows the AIMD simulations of catechol-double styrene, phenol-double styrene and benzene-double styrene with total binding energies 90 meV, 260 meV and 120 meV, respectively. Obtaining the lowest total binding energy (90 meV) in the system of catechol-double styrene could be explained due to the higher hydrophilicity of catechol compared to the others. On the other hand, the benzene ring with higher hydrophobicity showed only a slightly better binding property (120 meV) to the styrene rings. Much higher binding energy was observed for the phenol-double styrene system (260 meV) than the other two systems. In the absence of water, externally tilted styrene structure which induced the binding was observed only after addition of phenol. This showed that both hydroxyl group and benzene ring collaborate together to bind to styrene rings in the absence of water.

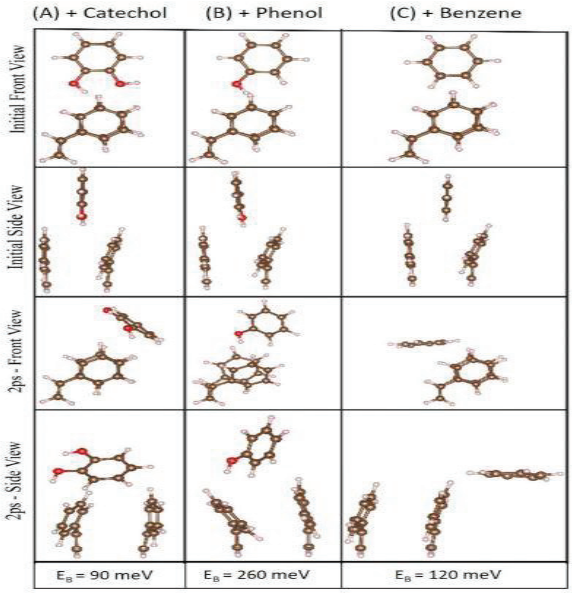


Figure 3. 8. AIMD simulations of the systems without water: initial and after 2 ps configurations with front and side views for the different systems composed of (A) two styrene and one catechol, (B) two styrene and one phenol and (C) two styrene and one benzene. Total binding energies of the systems are shown under the views. Red, white and brown atoms represent oxygen, hydrogen and carbon atoms, respectively.

The combined results of EPR measurements and DFT calculations provide the importance of hydroxyl groups on the wet adhesion of DOPA/tyrosine to PS surface. Semoto et al. have showed the role of hydroxyl groups and adsorbed water molecules in the adhesion interface between a fragment of epoxy resin and a water adsorbed aluminum oxide surface by using DFT calculations (Semoto et al., 2012). The results demonstrated that the hydrogen-bond network via adsorbed water molecules significantly affects the adhesion mechanism. Here, in water, externally tilted styrene conformation enhances the interaction between DOPA/tyrosine with styrene rings. Hydroxyl groups on the DOPA and tyrosine interact with water molecules via hydrogen bonding, and move together which enhances the adhesion on PS. However, phenylalanine without hydroxyl groups could not interact with water. So, in the presence of water, pre-adsorbed water molecules on the styrene surface do not allow phenylalanine to be close to the styrene surface. This is also supported with the AIMD simulations of the systems in the absence of water.

Without water, styrene rings externally tilted with respect to each other only with phenol addition which increases the binding. Hydrophilic and hydrophobic interactions together determine the binding of catechol to the styrene surface.

# CHAPTER 4

# CONCLUSION

In the literature, the role of DOPA hydroxyl groups in the wet adhesion to the hydrophilic surfaces e.g. silica, mica and glass was investigated in detail. However, the role of DOPA hydroxyl groups in the wet adhesion to the hydrophobic surface was not studied before. Here, we experimentally and theoretically investigated the effects of hydroxyl groups on the wet adhesion to the hydrophobic polystyrene (PS) surface. Three amino acids with similar structures except the number of their hydroxyl groups, DOPA, tyrosine and phenylalanine, were attached to the four chain ends of a PEG polymer; PEG-(N-Boc-L-DOPA)$_4$, PEG-(N-Boc-L-Tyrosine)$_4$ and PEG-(N-Boc-L-Phenylalanine)$_4$. Their wet adhesive properties were compared by using EPR spectroscopy in terms of their surface coverages. Spin labeled polystyrene (SL-PS) was prepared in water to be used as a model surface for the EPR measurements. Without applying force, PEG-(N-Boc-L-DOPA)$_4$ and PEG-(N-Boc-L-Tyrosine)$_4$ were able to adhere to SL-PS surfaces with the percentages of surface coverages 70% and 50%, respectively. However, PEG-(N-Boc-L-Phenylalanine)$_4$ did not adhere to the SL-PS surface noticeably. This showed that hydroxyl groups on the benzene rings enhance the adhesion to PS in water. In addition, the spontaneous wet adhesion was not achieved by phenylalanine without having a hydroxyl group on the benzene side.

To further confirm the hydroxyl group effects on the wet adhesion, DFT calculations were applied to the systems including two water molecules and double styrene rings. For the DFT calculations, catechol, phenol and benzene molecules were used instead of DOPA, tyrosine and phenylalanine, respectively. After addition each of these molecules to the double styrene - double water systems, the system binding energies increases in the order of benzene < phenol < catechol with energies 562 meV, 733 meV and 762 meV. This result is in parallel with the result obtained from the EPR measurements that showed the similar but better adhesion of DOPA than tyrosine, and also not a significant adhesion of phenylalanine to the PS surface. In water, the better adhesions of DOPA and tyrosine than phenylalanine to PS surface could be due to the formed hydrogen bonds between DOPA/ tyrosine and water molecules. Pre-adsorbed

water molecules on styrene induce DOPA/tyrosine to be more interactive with styrene rings through π-π stacking. However, phenylalanine without hydroxyl group does not interact with water on the styrene surface and cannot be close enough to achieve strong bindings with styrene. In addition, in the absence of water, DFT calculations showed that finding one hydroxyl group on the phenol enhances the interaction between phenol and styrenes more than the interactions between catechol-styrenes and benzene-styrenes in the order of catechol < benzene < phenol.

# REFERENCES


Akdogan, Y.; Synthesis, Characterization and Chemical Behaviour of Small Paramagnetic Pt Species Inside Zeolites Studied by EPR, XAS and FTIR. Ph. D. Thesis, University of Stuttgart 2009.

Akdogan, Y.; Wei, W.; Huang, K.Y.; Kageyama, Y.; Danner, E.W.; Miller, D.R.; Rodriguez, N.R.M.; Waite, J.H.; Han, S. Intrinsic Surface-Drying Properties of Bioadhesive Proteins. Angewandte Chemie International Edition 2014, 126, 11435–11438.

Akdogan, Y.; Emrullahoglu, M.; Tatlıdil, D.; Ucuncu, M.; Cakan-Akdogan, G. EPR Studies of Intermolecular Interactions and Competitive Binding of Drugs in a Drug–BSA Binding Model. Physical Chemistry Chemical Physics 2016, 18, 22531–22539.

Antosiewicz, J.M.; Shugar, D. UV–Vis Spectroscopy of Tyrosine Side-Groups in Studies of Protein Structure. Part 2: Selected Applications. Biophysical Reviews 2016, 8, 163–177.

Cencer, M.; Liu, Y.; Winter, A.; Murley, M.; Meng, H.; Lee, B.P. Effect of pH on the Rate of Curing and Bioadhesive Properties of Dopamine Functionalized Poly(ethylene glycol) Hydrogels. Biomacromolecules 2014, 15, 2861–2869.

Chen, S.-K.; Wang, B.-C.; Zhou, T.-G.; Huang, W.-Z. Theoretical Study of the Adsorption of DOPA-Quinone and DOPA-Quinone Chlorides on Cu (100) Surface. Applied Surface Science 2011, 257, 7938–7943.

Dalsin, J.L.; Hu, B.H.; Lee, B.P.; Messersmith, P.B. Mussel Adhesive Protein Mimetic Polymers for the Preparation of Nonfouling Surfaces. Journal of the American Chemical Society 2003, 125,4253-4258.

Das P.; and Reches, M.; Revealing the Role of Catechol Moieties in the Interactions Between Peptides and Inorganic Surfaces. Nanoscale 2016, 8, 15309.

Eberle, N.; Lee, B.; Messersmith, P.B.; Westhaus, E.; Zeng, X. Synthesis and Characterization of DOPA-PEG Conjugates. Polymer Preprints 2000, 1, 989-990.

Forooshani, P.K.; Lee, B.P. Recent Approaches in Designing Bioadhesive Materials Inspired by Mussel Adhesive Protein. Journal of Polymer Science Part A: Polymer Chemistry 2017, 55, 9–33.

Gao, Z.; Duan, L.; Yang, Y.; Hu, W.; Gao, G. Mussel-Inspired tough Hydrogels with Selfrepairing and Tissue Adhesion., Applied Surface Sciece 2018, 427, 74–82.

Giorgioni, G.; Claudi, F.; Ruggieri, S.; Ricciutelli, M.; Palmieri, G.F.; Di Stefano, A.; Sozio, P.; Ceresa, L.S.; Chiavaroli, A.; Ferrante, C.; Orlando, G.; Glennon, R.A. Design, Synthesis, and Preliminary Pharmalogical Evaluation of New Imidazolinon-es as L-DOPA Prodrugs. Bioorganic Medicinal Chemistry 2010, 18, 1834-1843.

Göksel, Y.; Kırpat, I.; Akdogan, Y. Spontaneous Adhesion of DOPA and Tryptophan Functionalized PEG to Polystyrene Nanobeads: an EPR Study. Materials Science Forum 2018, 243-247.

Göksel, Y.; Akdogan, Y. Increasing Spontaneous Wet Adhesion of DOPA with Gelation Characterized by EPR Spectroscopy. Materials Chemistry and Physics 2019, 124–130.

Grimme, S.; Ehrlich, S.; Goerigk, L. Effect of the Damping Function in Dispersion Corrected Density Functional Theory. Journal of Computational Chemistry 2011, 32, 1456–1465.

Guvendiren, M.; Messersmith, P.B.; Shull, K.R.; Self-Assembly and Adhesion of DOPA Modified Methacrylic Triblock Hydrogels. Biomacromolecules 2008, 9, 122-128.

Heo, J.; Kang, T.; Jang, S.G.; Hwang, D.S.; Spruell, J.M.; Killops, K.L.; Waite, J.H.; Hawker, C.J. Improved Performance of Protected Catecholic Polysiloxanes for Bioinspired Wet Adhesion to Surface Oxides. Journal of the American Chemical Society 2012, 134,20139-20145.

Hinderberger, D.; Jeschke, G. Site-Specific Characterization of Structure and Dynamics of Complex Materials by EPR Spin Probes. Modern Magnetic Resonance 2008, 1529-1537.

Hinderberger, D. EPR Spectroscopy in Polymer Science. Current Chemistry Letters 2011, 321: 67-90.

Hwang, D.S.; Gim, Y.; Yoo, H.J.; Cha, H.J.; Practical Recombinant Hybrid Mussel Bioadhesive fp-151. Biomaterials 2007, 28, 3560-3568.

Kattnig, D. R.; Akdogan, Y.; Bauer, C.; Hinderberger, D. High-Field EPR Spectroscopic Characterization of Spin Probes in Aqueous Ionic Liquid Mixtures. Zeitschrift für Physikalische Chemie 2012, 226, 1363-1378.

Kattnig, D. R.; Akdogan, Y.; Lieberwirth, I.; Hinderberger, D. Spin Probing of Supramolecular Structures in 1-butyl-3-methyl-imidazolium Tetrafluoroborate/water Mixture. Molecular Physics 2013, 111, 2723-2737.

Kirpat, I. Obtaining Underwater Adhesive Materials and Characterization of Their Adhesive Properties to Different Surfaces by ESR Spectroscopy MSc. Thesis, İzmir Institute of Technology 2016.

Kırpat, I.; Goksel, Y.; Karakus, E.; Emrullahoglu, M.; Akdogan, Y. Determination of Force-Free Wet Adhesion of Mussel-Inspired Polymers to Spin Labeled Surface. Materials Letters 2017, 48–51.

Kresse, G.; Furthmüller, J. Efficient Iterative Schemes for ab Initio Total-Energy Calculations Using a Plane-Wave Basis Set. Physical Review B 1996, 54, 11169.

Laulicht, B.; Mancini, A.; Geman, N.; Cho, D.; Estrellas, K.; Furtado, S.; Hopson, R.; Tripathi, A.; Mathiowitz, E. Bioinspired Bioadhesive Polymers: Dopa-Modified Poly(acrylic acid) Derivatives. Macromolecular Bioscience 2012, 12, 1555-1565.

Lee, B.P.; Dalsin, J.L.; Messersmith, P.B. Synthesis and Gelation of DOPA-Modified Poly(ethylene glycol) Hydrogels. Biomacromolecules 2002, 3, 1038–1047.

Lee, B.P.; Chao, C.Y.; Nunalee, F.N.; Motan, E.i.; Shull, K.R.; Messersmith, P.B. Rapid Gel Formation and Adhesion in Photocurable and Biodegradable Block Copolymers with High DOPA Content. Macromolecules 2006, 39, 1740-1748.

Lee, B.P.; Messersmith, P.B.; Israelachvili, J.N.; Waite, J.H.; Mussel-Inspired Adhesives and Coatings.Annual Review of Materials Research 2011, 41:99–132.

Leng, C.; Liu, Y.; Jenkins, C.; Meredith, H.; Wilker, J.J.; Chen, Z. Interfacial Structure of a DOPA- Inspired Adhesive Polymer Studied by sum Frequency Generation Vibrational Spectroscopy. Langmuir 2013, 29, 6659–6664.

Levine, Z.A.; Rapp, M.V.; Wei, W.; Mullen, R.G.; Wu, C.; Zerze, G.H.; Mittal, J.; Waite, J. H.; Israelachvili, J.N.; Shea, J.-E. Surface Force Measurements and Simulations of Mussel-Derived Peptide Adhesives on Wet Organic Surfaces. Proceedings of the National Academy of Sciences of the United States of America 2016, 113, 4332–4337.

Lin, Q.; Gourdon, D.; Sun, C.; Holten-Anderson, N.; Anderson, T.H.; Waite, J.H.; Israelachvili, J.N. Adhesion Mechanisms of the Mussel Foot Proteins mfp-1 and mfp-3. Proceedings of the National Academy of Sciences of the United States of America (PNAS) 2007, 104 (10) 3782-3786.

Lu, Q.; Danner, E.; Waite, J.H.; Israelachvili, J.N.; Zeng, H.; Hwang, D.S. Adhesion of Mussel Foot Proteins to Different Substrate Surfaces. Journal of Royal Society Interface 2013, 10:20120759.

Matos-Perez, C.R.; White, J.D.; Wilker, J.J. Polymer Composition and Substrate Influences on the Adhesive Bonding of a Biomimetic, Cross-Linking Polymer. Journal of American Chemical Society 2012, 134, 9498-9505.

Mian, S.A.; Saha, L.C.; Jang, J.; Wang, L.; Gao, X.; Nagase, S. Density Functional Theory Study of Catechol Adhesion on Silica Surfaces. The Journal of Physical Chemistry C 2010, 114, 20793–20800.

Mueller, C.; Capalle, M.A.H.; Arvinte, T.; Seyrek, E.; Borchard, G. Tryptophan mPEGs: Novel Excipients that Stabilize Salmon Calcitonin against Aggregation by Noncovalent PEGylation. European Journal of Pharmaceutics and Biopharmaceutics. 2011, 79, 646-657.

Perdew, J.P.; Burke, K.; Ernzerhof, M. Generalized Gradient Approximation Made Simple. Physical Review Letter 1996, 77, 3865.

Semoto, T.; Tsuji, Y.; Yoshizawa, K. Molecular Understanding of The Adhesive Force Between a Metal Oxide Surface and an Epoxy Resin: Effects of Surface Water. Bulletin of the Chemical Society of Japan 2012, 85, 672–678.

Stoll, S.; Schweiger, A. EasySpin, a Comprehensive Software Package for Spectral Simulation and Analysis in EPR. Journal of Magnetic Resonance 2006, 178, 42–55.

Talsi, E.P.; Bryliakov, K. Applications of EPR and NMR Spectroscopy in Homogeneous Catalysis. CRC Press: Boca Raton, FL, 2017.

Tatlidil, D.; Ucuncu, M.; Akdogan, Y.; Physiological Concentrations of Albümin Favor Drug Binding. Physical Chemistry Chemical Physics 2015, 17, 22678-22685.

Tretinnikov, O.N. Hydrophilic (Hydrogen-Bonding) Polystyrene Surface by Substrate-Induced Surface Segregation of Benzene Groups. Langmuir 2000, 16, 2751–2755.

Waite, J.H. Mussel Adhesion – Essential Footwork. Journal of Experimental Biology 2017, 220, 517–530.

Wang, J.J.; Tahir, M.N.; Kappl, M.; Tremel, W.; Metz, N.; Barz, M.; Theato, P.; Butt, H.J. Influence of Binding-Site Density in Wet Bioadhesion. Advanced Materials 2008, 20, 3872-3876.

Yang, B.; Lim, C.; Hwang, D.S.; Cha, H.J. Switch of Surface Adhesion to Cohesion by DOPA-$Fe^{3+}$ Complexation, in Response to Microenvironment at the Mussel Plaque/ Substrate Interface. Chemistry of Materials 2016, 28, 7982–7989.

Yildiz, R.; Ozen, S.; Sahin, H.; Akdogan, Y. The Effect of DOPA Hydroxyl Groups on Wet Adhesion to Polystyrene Surface: An Experimental and Theoretical Study. Materials Chemistry and Physics 2020, 243, 122606.

Yu, J.; Wei, W.; Danner, E.; Israelachvili, J.N.; Waite, J.H. Effects of Interfacial Redox in Mussel Adhesive Protein Films on Mica. Advanced Materials 2011, 23, 2362-2366.

Zeng, X.; Westhaus, E.; Eberle, N.; Lee, B.; Messersmith, B.P. Synthesis and Characterization of DOPA-PEG Conjugates. Polymer Preprints 2000, 41(1), 989.

Zhang, W.; Yang, H.; Liu, F.; Chen, T.; Hu, G.; Guo, D.; Hou, Q.; Wu, X.; Su, Y.; Wang, J. Molecular Interactions Between DOPA and Surfaces with Different Functional Groups: A Chemical Force Microscopy Study. Royal Society of Chemistry (RCS) Advances. 2017, 7, 32518–32527.

# APPENDIX

# $^{1}$H-NMR SPECTRA OF COMPOUNDS

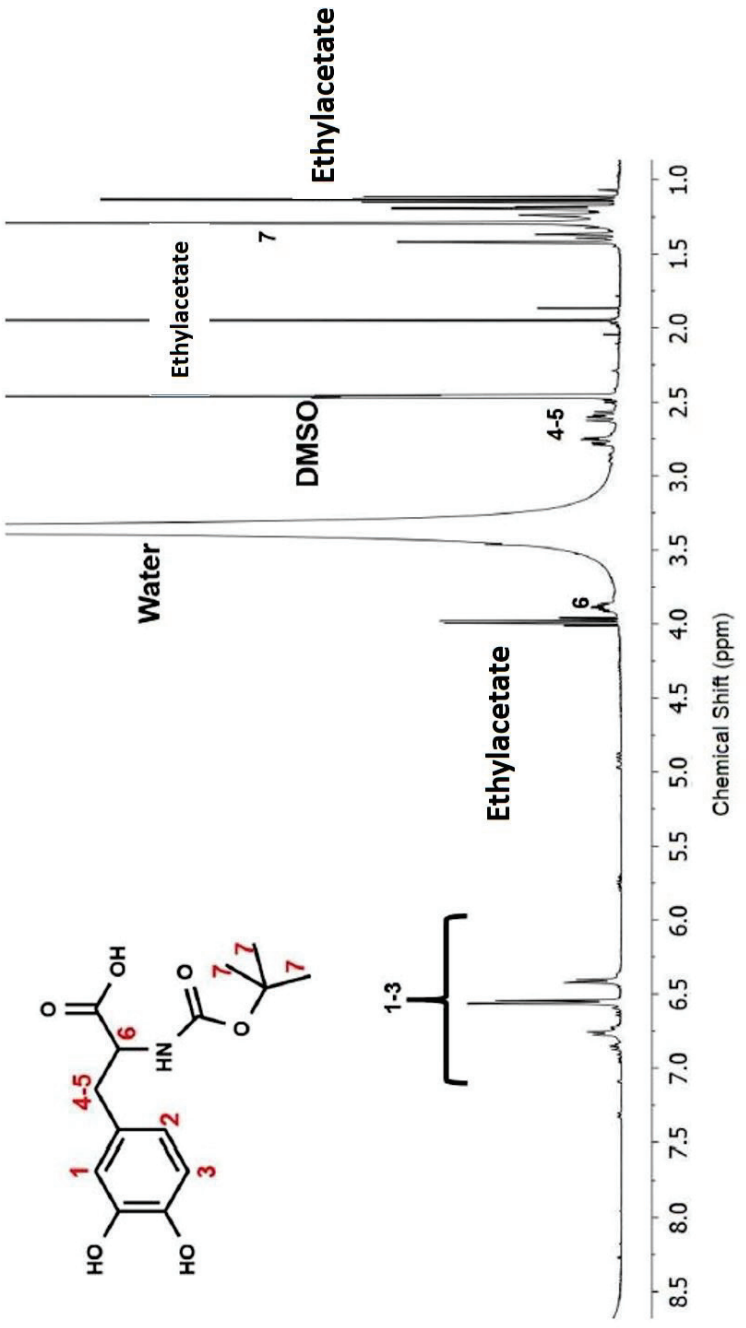


Figure A.1. $^{1}$H NMR of N-Boc-L-DOPA molecule.

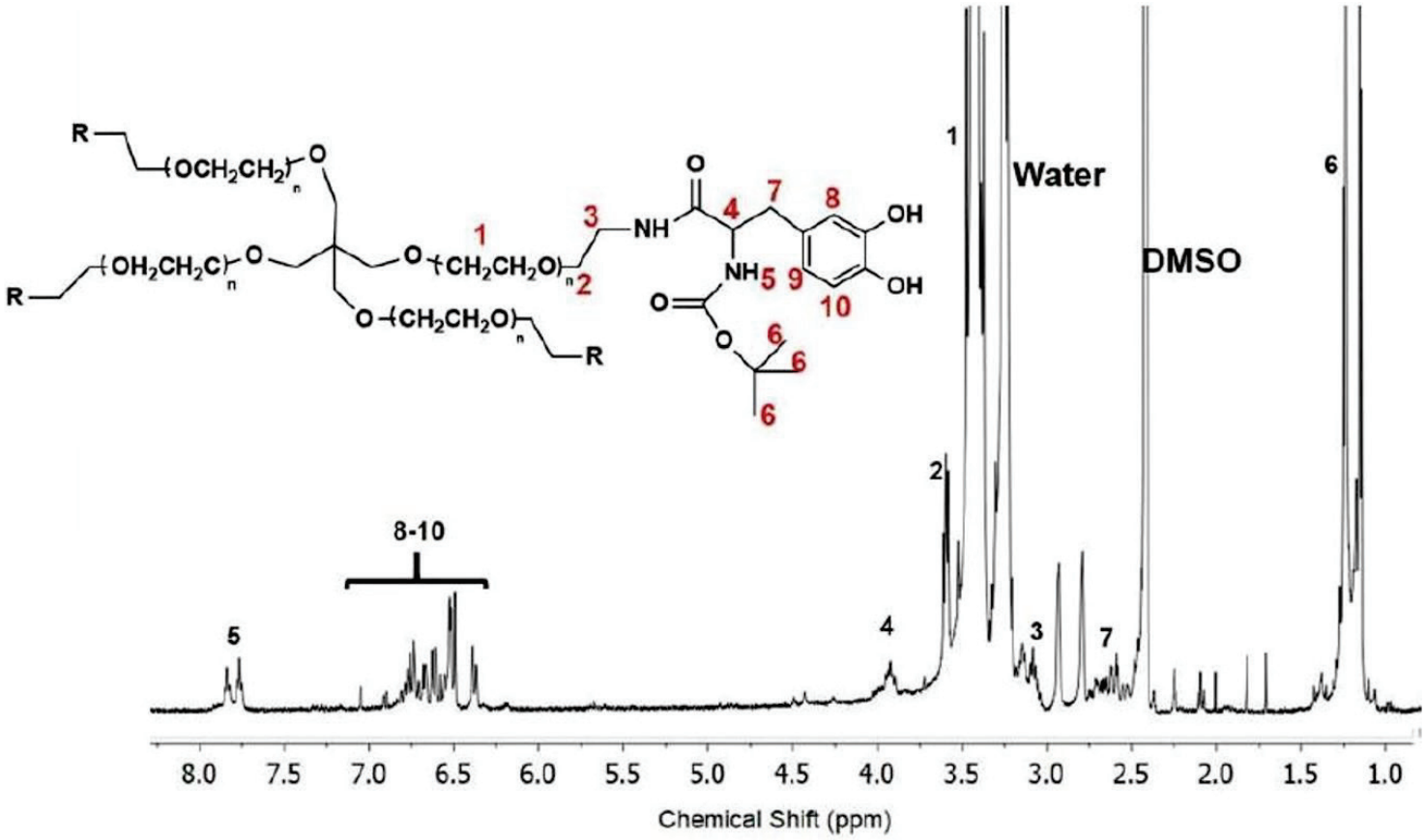


Figure A.2. $^{1}$H NMR of PEG-(N-Boc-L-DOPA)$_4$ molecule.

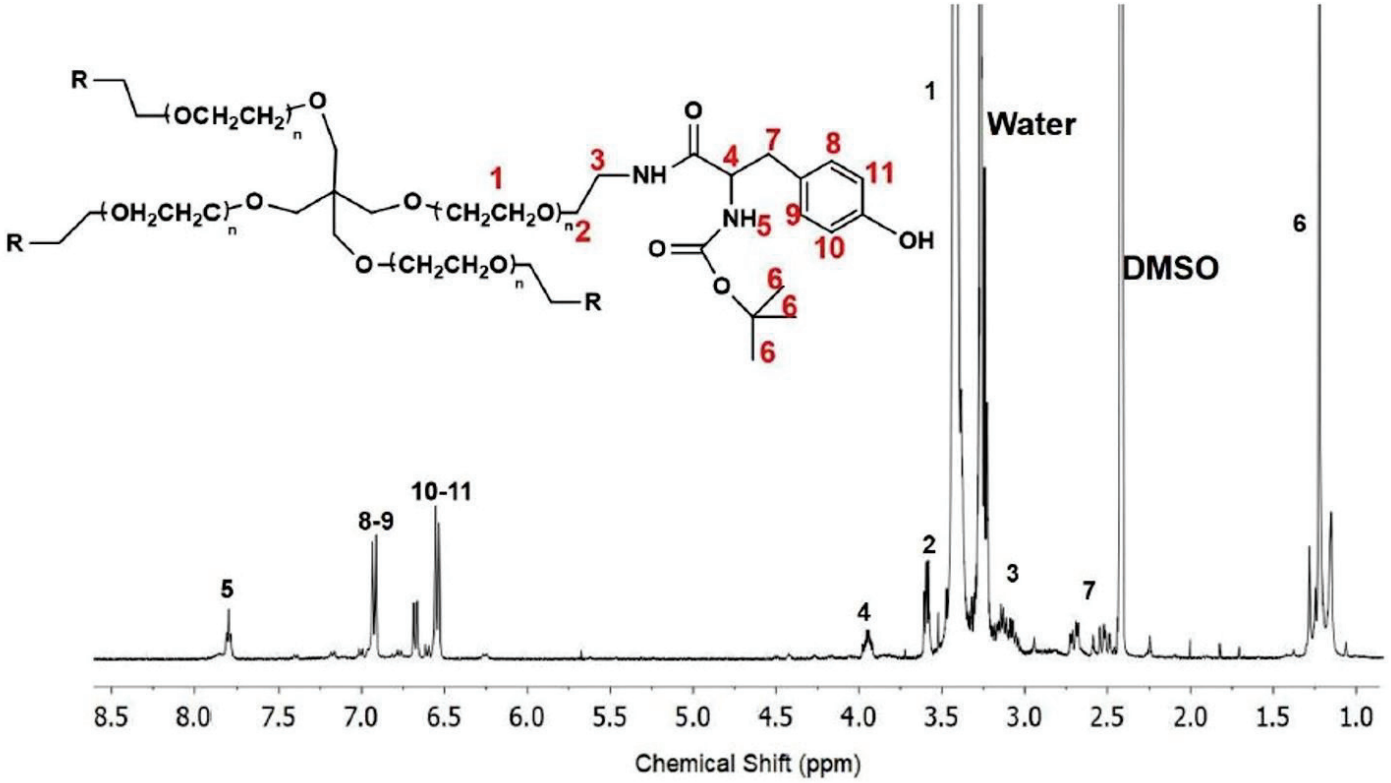


Figure A.3. $^{1}$H NMR of PEG-(N-Boc-L-Tyrosine)$_4$ molecule.

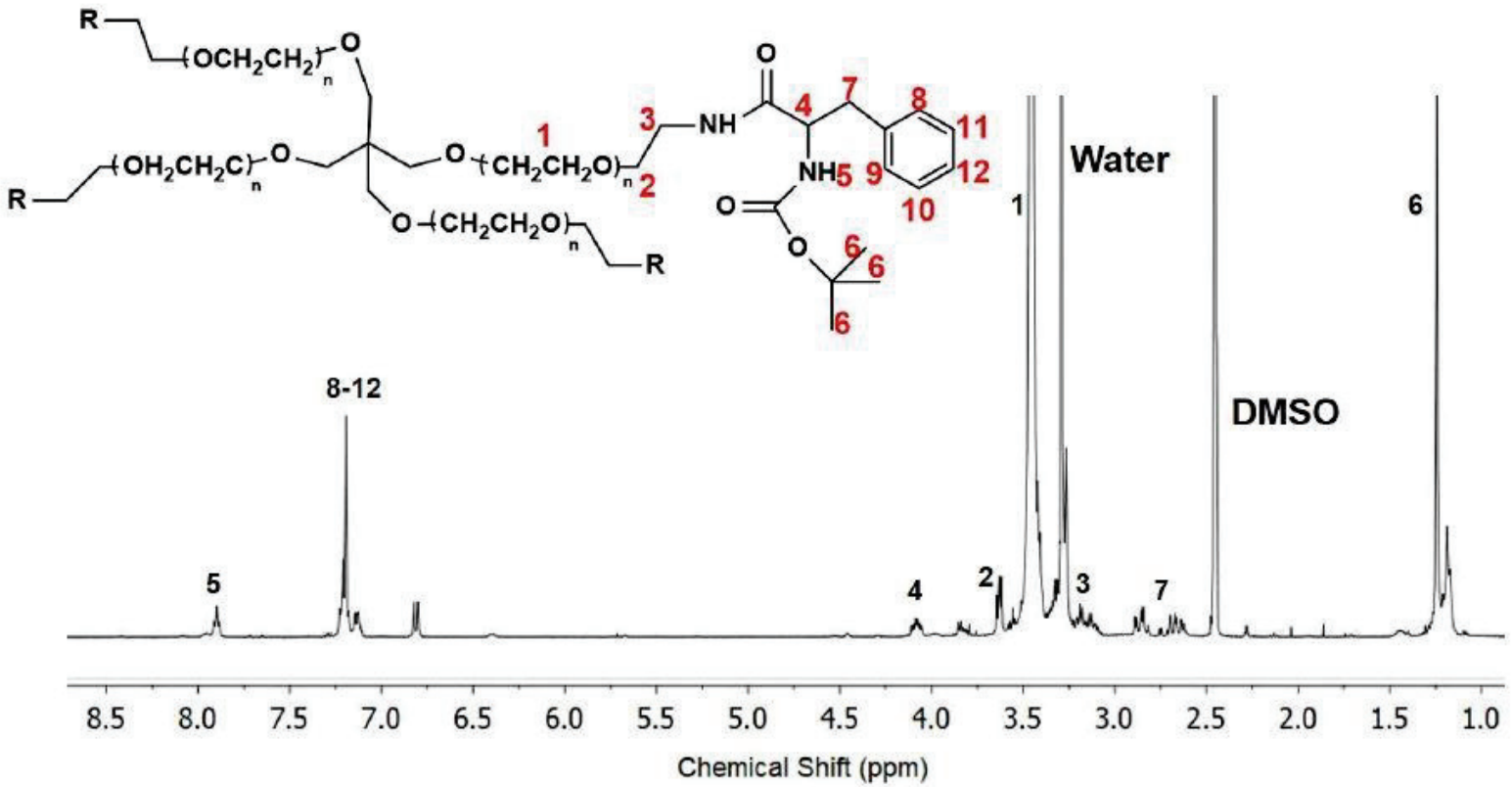


Figure A.4. $^{1}$H NMR of PEG-(N-Boc-L-Phenylalanine)$_4$ molecule.

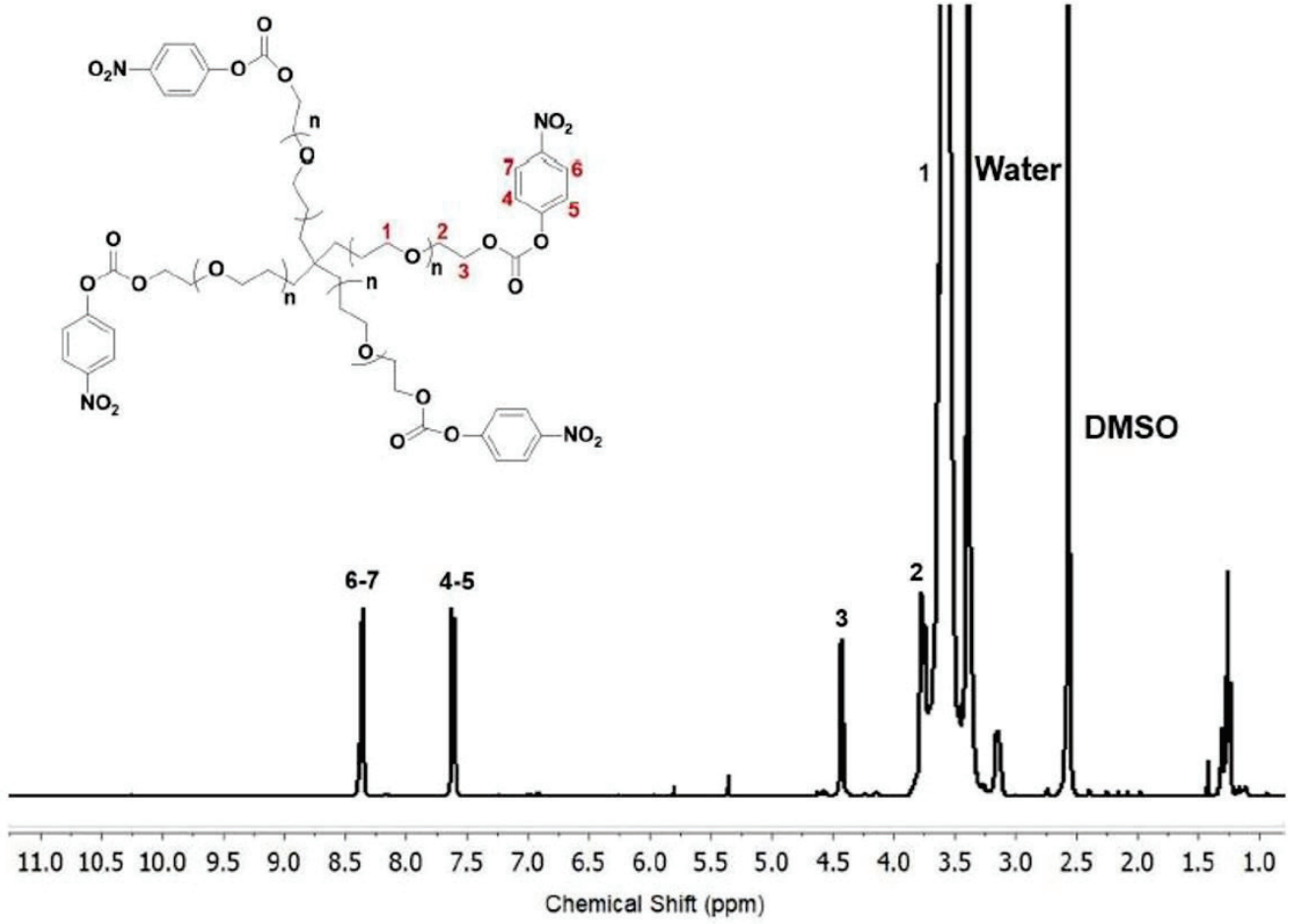


Figure A.5. $^{1}$H NMR of PEG-(p-nitrophenylcarbonate)$_4$ molecule.

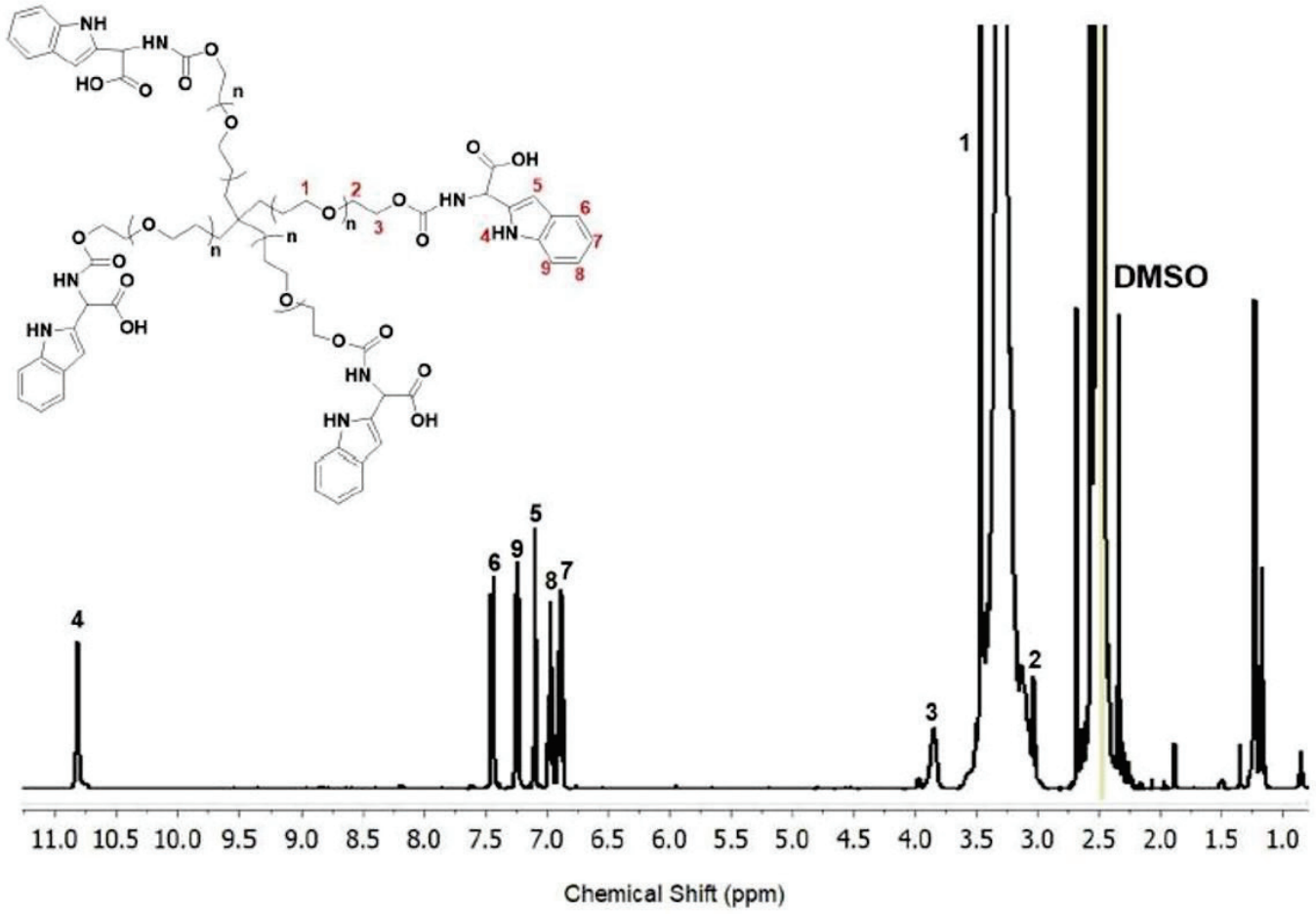


Figure A.6. $^{1}H$ NMR of PEG-$(Trp)_4$ molecule.

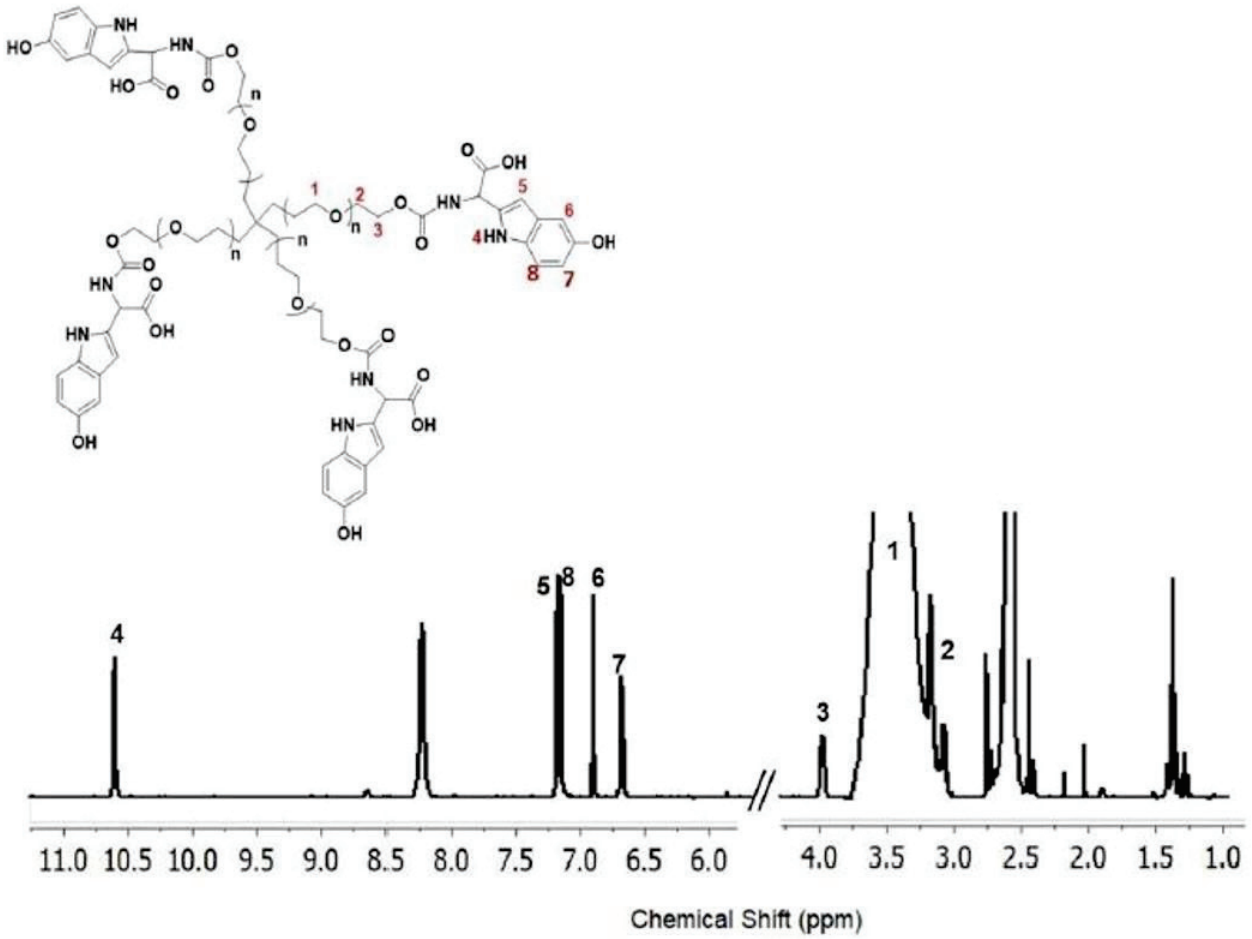


Figure A.7. $^{1}$H NMR of PEG-(5-HydroxyTryptophan)$_4$ molecule.